SCIENTIFIC REPORTS

OPEN

Aerobic exercise and a BDNF-mimetic therapy rescue learning and memory in a mouse model of Down syndrome

Received: 14 June 2017
Accepted: 23 November 2017
Published online: 04 December 2017

Martina Parrini[1], Diego Ghezzi[1,4], Gabriele Deidda[1,6], Lucian Medrihan[1,5], Enrico Castroflorio[2], Micol Alberti[1], Pietro Baldelli[2,3], Laura Cancedda[1] & Andrea Contestabile[1]

Down syndrome (DS) is caused by the triplication of human chromosome 21 and represents the most frequent genetic cause of intellectual disability. The trisomic Ts65Dn mouse model of DS shows synaptic deficits and reproduces the essential cognitive disabilities of the human syndrome. Aerobic exercise improved various neurophysiological dysfunctions in Ts65Dn mice, including hippocampal synaptic deficits, by promoting synaptogenesis and neurotransmission at glutamatergic terminals. Most importantly, the same intervention also prompted the recovery of hippocampal adult neurogenesis and synaptic plasticity and restored cognitive performance in trisomic mice. Additionally, the expression of brain-derived neurotrophic factor (BDNF) was markedly decreased in the hippocampus of patients with DS. Since the positive effect of exercise was paralleled by increased BDNF expression in trisomic mice, we investigated the effectiveness of a BDNF-mimetic treatment with 7,8-dihydroxyflavone at alleviating intellectual disabilities in the DS model. Pharmacological stimulation of BDNF signaling rescued synaptic plasticity and memory deficits in Ts65Dn mice. Based on our findings, Ts65Dn mice benefit from interventions aimed at promoting brain plasticity, and we provide evidence that BDNF signaling represents a potentially new pharmacological target for treatments aimed at rescuing cognitive disabilities in patients with DS.

Down syndrome (DS) is the main cause of genetically defined intellectual disability, with an estimated frequency of 1 in every 1000 live births[1]. Intellectual disabilities represent the major hallmark of DS and are characterized by a low Intelligence Quotient (IQ), as well as learning and memory deficits in different cognitive domains[1–4]. The Ts65Dn mouse is the best characterized and most widely used animal model of DS. It carries a freely segregating extra chromosome bearing the triplication of the distal segment of mouse chromosome 16, which is syntenic to part of the long arm of human chromosome 21[5]. The Ts65Dn mouse recapitulates many aspects of DS, including cognitive impairment and altered hippocampus-dependent memory function[5–7]. Although the Ts65Dn model presents some genetic limitations due to partial triplication of human chromosome 21 (HSA21) orthologous genes and the concurrent triplication of some non-HSA21 genes[8], it recapitulates many of the phenotypic features of the human syndrome and is currently the only mouse model used for preclinical identification of pharmacological interventions targeting cognitive impairments in DS[9]. A number of mechanisms underlying these cognitive hallmarks have been identified in Ts65Dn mice, including an imbalance between excitatory and inhibitory neurotransmission[10–19], impairment of hippocampal synaptic plasticity[6,11,20] and a decrease in adult neurogenesis in the hippocampal dentate gyrus (DG)[6,21].

[1]Department of Neuroscience and Brain Technologies, Istituto Italiano di Tecnologia, Genova, Italy. [2]Center for Synaptic Neuroscience, Istituto Italiano di Tecnologia, Genova, Italy. [3]Department of Experimental Medicine, University of Genova, Genova, Italy. [4]Present address: Medtronic Chair in Neuroengineering, Center for Neuroprosthetics, Institute of Bioengineering, School of Engineering, École Polytechnique Fédérale de Lausanne, Lausanne, Switzerland. [5]Present address: Laboratory of Molecular and Cellular Neuroscience, Rockefeller University, New York, NY, USA. [6]Present address: Laboratory of Neurophysiology, Department of Physiology and Biochemistry, University of Malta, Msida, Malta. Correspondence and requests for materials should be addressed to A.C. (email: andrea.contestabile@iit.it)

According to previous studies of both rodents and humans, aerobic exercise induces a wide range of beneficial effects on brain neurophysiology, including enhanced expression of neurotrophins, increased hippocampal volume and improved cognitive performance[22–39]. The beneficial effects of aerobic exercise have been associated with the upregulation of BDNF expression, increased adult neurogenesis in the hippocampal DG and potentiation of synaptic plasticity[23–25,29–33,40–48]. Indeed, among the many molecular players involved in the positive effect of exercise, BDNF signaling through its tropomyosin-receptor-kinase B (TrkB) receptor is known to play a pivotal role in both enhanced brain plasticity and cognition[47,49–52]. Moreover, many studies have highlighted BDNF/TrkB signaling as a main regulator of long-term potentiation (LTP, a well characterized model of synaptic plasticity) at hippocampal Schaffer collateral-CA1 synapses[53–55], hippocampus-dependent cognition and learning[56–62] and the maturation and integration of DG newborn neurons into the hippocampal circuit[63,64]. Interestingly, different manipulations that are able to rescue learning deficits in Ts65Dn mice are associated with increased BDNF expression[17,65–67], indicating a possible common mechanism of action through the modulation of the neurotrophin system.

Here, we report a detailed biochemical, structural, electrophysiological and behavioral assessment of the positive effect of aerobic exercise on the corresponding deficits observed in trisomic animals, indicating that exercise is a valuable tool to promote brain plasticity and possibly represents a complementary therapeutic approach to pharmacologic interventions in patients with DS. Interestingly, BDNF expression was substantially decreased in the hippocampus of patients with DS, and exercise increased BDNF expression in trisomic animals. Therefore, we investigated the use of a possible pharmacological approach intended to promote BDNF signaling in patients with DS and provide evidence that the treatment of Ts65Dn mice with the BDNF-mimetic drug 7,8-dihydroxyflavone (DHF), completely rescued learning and memory impairments. Thus, we identified a new pharmacological target to treat DS-associated cognitive impairment.

Results

In this study, we aimed to investigate the effects of strategies that stimulate brain neuroplasticity mechanisms on the rescue of learning and memory deficits observed in the Ts65Dn mouse model of DS. To accomplish this goal, we first took advantage of voluntary exercise, a paradigm known to promote plastic changes and exert beneficial effects on several neurochemical and functional aspects of both the human and rodent brains[22–24]. We hypothesized that aerobic exercise stimulates different neurophysiological processes in the trisomic brain, including adult neurogenesis, synaptogenesis, synaptic plasticity and neurotrophin expression. We provided adult Ts65Dn male mice and wild-type (WT) littermates (4-5 month-old) with free access to running wheels for 4 weeks to assess the effects of physical exercise on these different processes and on cognitive functions in the mouse model of DS (Fig. 1A). Control (sedentary) mice were housed in standard cages without running wheels. Both WT and Ts65Dn mice in the running group (exercise) showed strong running activity that was slightly, but significantly, higher for trisomic animals (WT: 4.33 ± 1.08 Km/day, $n = 14$; Ts65Dn: 5.56 ± 0.80 Km/day, Fig. 1A).

Aerobic exercise rescued learning and memory deficits in Ts65Dn mice. Based on accumulating evidence, physical exercise induces specific changes in neural function and enhances learning and memory, particularly hippocampus-dependent behaviors. According to previous behavioral studies, Ts65Dn mice exhibit learning and memory deficits in several behavioral tasks[5–7,10]. We tested Ts65Dn mice in a battery of behavioral tests to evaluate the long-term effects of aerobic exercise on different cognitive domains. Importantly, the exercise paradigm did not cause a general enhancement of motor performance (Supplementary Fig. 1) that could interfere with the evaluation of cognitive functions. We first used the contextual fear conditioning (CFC) test to evaluate associative memory. Consistent with the results from previous studies[6,7], sedentary Ts65Dn mice showed a strong reduction in the freezing response upon re-exposure to the adverse contest 24 hours after conditioning, indicating an impairment in associative learning in this test. Interestingly, exercise completely restored associative learning in Ts65Dn mice (Fig. 1B), without inducing changes in non-associative freezing (*i.e.*, exposure to a new context) or altering sensitivity to the shock (Supplementary Fig. 2A).

Next, we evaluated the effect of exercise on spatial memory with the object location (OL) test. In this test, mice must discriminate the new location of a familiar object in relation to the available spatial information. Sedentary Ts65Dn mice were unable to identify the new location after a retention period of 24 hours. However, after 4 weeks of exercise, the performance of Ts65Dn mice was indistinguishable from WT mice, indicating the complete recovery of spatial memory in trisomic animals (Fig. 1C). Next, we used the novel object recognition (NOR) test to evaluate long-term discriminative memory. As expected, sedentary Ts65Dn mice were unable to discriminate the new object, but performed as well as sedentary WT mice following the exercise paradigm (Fig. 1D). Notably, and consistent with other reports, exercise enhanced novel object recognition memory in WT mice[68,69]. The effect of exercise on Ts65Dn mice in both OL and NOR tests was independent of the preference for a different object (Supplementary Fig. 2B,C).

Aerobic exercise restores functional hippocampal adult neurogenesis in Ts65Dn mice. Adult neurogenesis in the DG is involved in hippocampus-dependent memory functions[70] and is known to be regulated by a variety of factors, such as age, stress, exercise, environment, learning, and seizures[46,48,70–72]. In particular, voluntary wheel-running robustly enhances cell proliferation and the number of newly generated neurons in the dentate subgranular zone (SGZ) of the hippocampus[43,46,48]. Since hippocampal cell proliferation and neurogenesis are impaired in adult Ts65Dn mice[6,21], we thus assessed whether voluntary aerobic exercise positively impacted adult hippocampal neurogenesis in Ts65Dn mice. We first evaluated the proliferation of neural progenitor cells (NPCs) in the DG by labeling dividing cells with the thymidine analog 5-bromo-2-deoxyuridine (BrdU) during the last week of wheel running exercise (Fig. 2A). As expected, the number of BrdU-positive cells ($BrdU^+$) cells was substantially decreased in sedentary Ts65Dn mice compared to WT mice, consistent with a

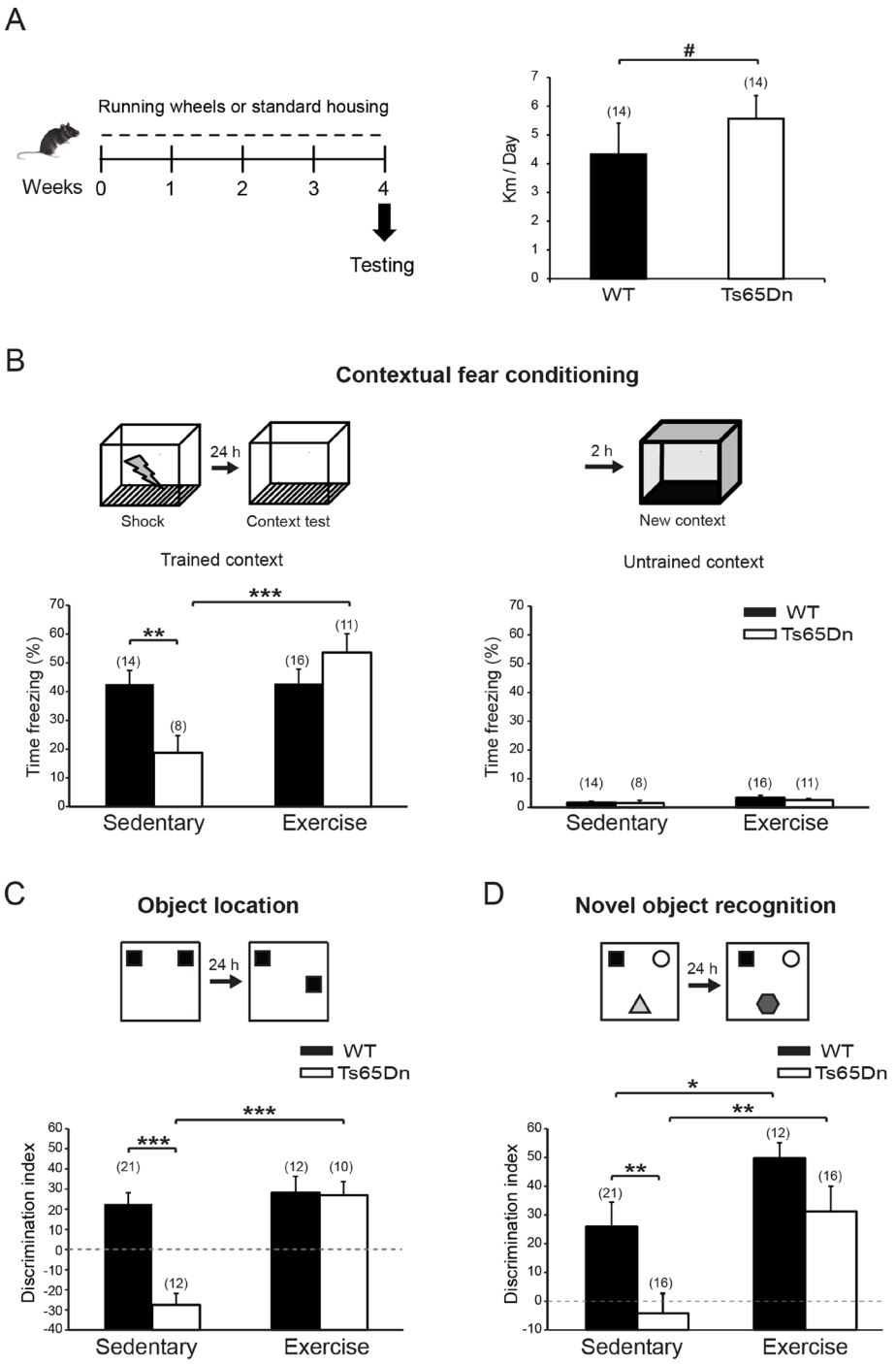

Figure 1. Physical exercise improved cognitive deficits in Ts65Dn mice. (**A**) *Left*, schematic representation of the experimental protocol. *Right*, average daily distance travelled by WT and Ts65Dn mice in the running group. $^{\#}P = 0.033$ Mann-Whitney Test. (**B**) *Top*, schematic representation of the contextual fear conditioning test. *Left*, sedentary Ts65Dn mice showed a strong reduction in freezing response in the context test, indicative of impaired associative learning. Physical exercise completely restored contextual learning in trisomic mice. Two-way ANOVA: genotype [$F_{1,45} = 1.353$, $P = 0.251$]; treatment [$F_{1,45} = 9.512$, $P = 0.003$]; genotype x treatment [$F_{1,45} = 9.322$, $P = 0.004$]. *Right*, both WT and Ts65Dn mice showed negligible freezing response when exposed to a new context. (**C**) *Top*, schematic representation of the object location (OL) test. *Bottom*, four weeks of physical exercise rescued spatial memory in Ts65Dn mice in the OL test. Two-way ANOVA: genotype [$F_{1,51} = 14.187$, $P < 0.001$]; treatment [$F_{1,51} = 19.382$, $P < 0.001$]; genotype x treatment [$F_{1,51} = 12.787$, $P < 0.001$]. (**D**) *Top*, schematic representation of the novel object recognition (NOR) test. *Bottom*, four weeks of physical exercise rescued novelty discrimination deficits in Ts65Dn mice in the NOR test. Two-way ANOVA: genotype [$F_{1,61} = 8.856$; $P = 0.004$]; treatment [$F_{1,61} = 13.114$; $P < 0.001$]; genotype x treatment [$F_{1,61} = 0.503$; $P = 0.481$]. For all panels the number in parenthesis indicates the number of animals tested for each experimental group. $^{*}P < 0.05$, $^{**}P < 0.01$, $^{***}P < 0.001$, Tukey *post hoc* test following two-way ANOVA.

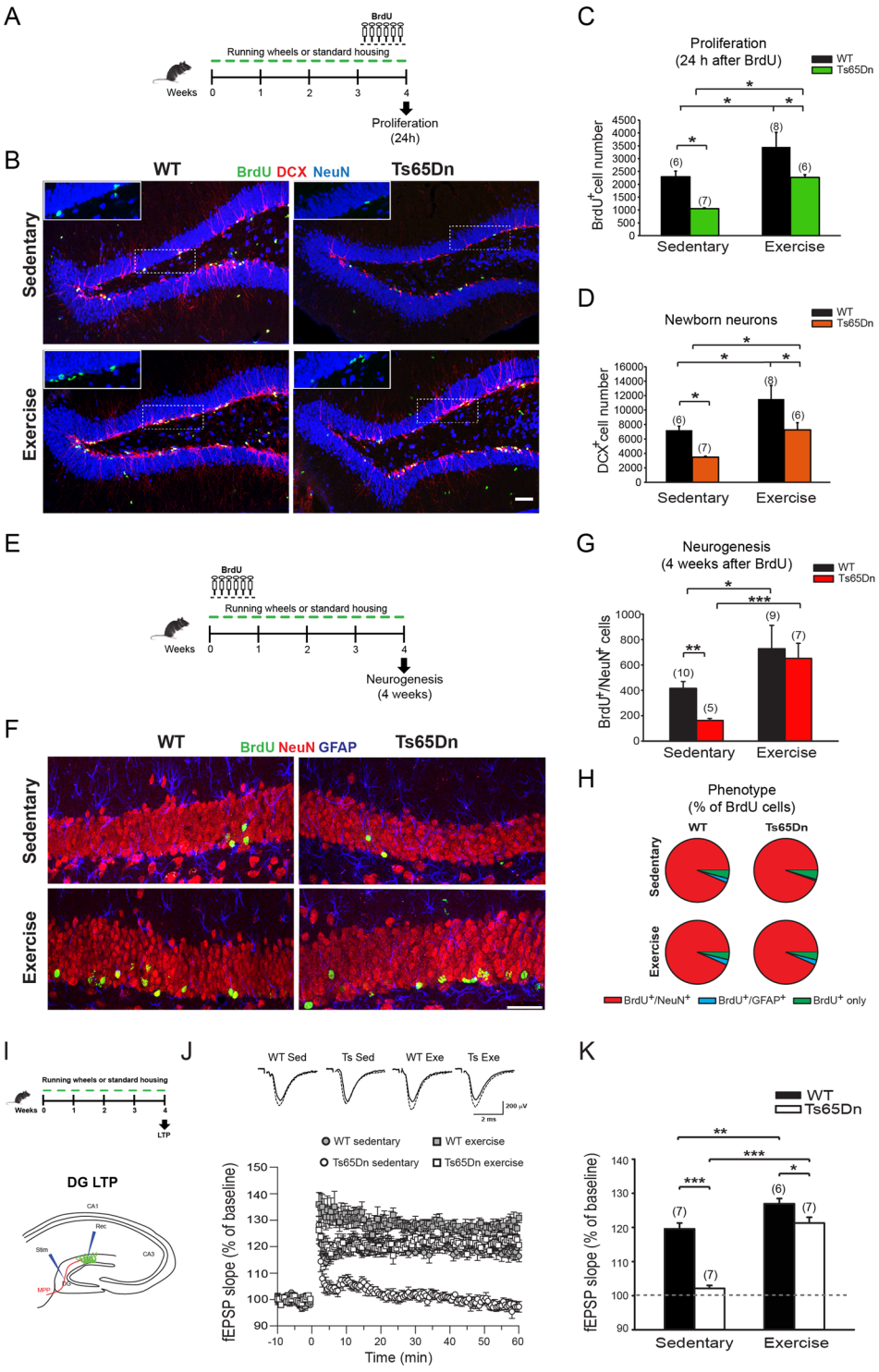

Figure 2. Voluntary exercise restored functional adult neurogenesis in the DG of Ts65Dn mice. (**A**) Schematic representation of the experimental protocol and BrdU administration to label proliferating cells. (**B**) Representative confocal z-stack projection images showing immunostaining for BrdU (green), DCX (red) and the pan-neuronal marker NeuN (blue). Scale bar: 50 µm. The insert on the upper-left corner of each image shows a detail of BrdU staining in the area indicated by the dashed rectangle. (**C**) Quantitative analyses of $BrdU^+$ cells found 24 h post BrdU administration in sedentary or running Ts65Dn and WT mice. Proliferation of neural precursor cells was fully rescued by exercise in Ts65Dn mice. Two-way ANOVA: genotype [$F_{1,23} = 10.967$, $P = 0.003$]; treatment [$F_{1,23} = 11.391$, $P = 0.003$]; genotype x treatment [$F_{1,23} = 0.0000291$, $P = 0.996$]. (**D**) Quantitative analysis of DCX^+ cells in sedentary or running Ts65Dn and WT mice. Numbers of DCX^+ immature newborn neurons were totally restored in Ts65Dn mice by running. Two-way ANOVA: genotype [$F_{1,23} = 10.244$, $P = 0.004$]; treatment [$F_{1,23} = 10.480$, $P = 0.004$]; genotype x treatment [$F_{1,23} = 0.0455$, $P = 0.833$]. (**E**) Schematic representation of the experimental protocol for BrdU pulse-chase experiments. (**F**)

Representative confocal z-stack projection images showing immunostaining for BrdU (green), NeuN (red) and GFAP (blue) on brain slices from mice sacrificed 4 weeks after BrdU administration. Scale bar: 50 µm. (**G**) The number of new neurons ($BrdU^+/NeuN^+$) found 4 weeks after BrdU administration was rescued by exercise in Ts65Dn mice. Two-way ANOVA: genotype [$F_{1,27} = 5.123$, $P = 0.032$]; treatment [$F_{1,27} = 22.833$, $P < 0.001$]; genotype x treatment [$F_{1,27} = 4.871$, $P = 0.036$]. (**H**) Percentage distribution of $BrdU^+/NeuN^+$, $BrdU^+/GFAP^+$, and $BrdU^+$ only-labeled cells found 4 weeks after BrdU administration. No statistical difference was found between the experimental groups. (**I**) Schematic representation of the experimental protocol and positioning of stimulating and recording electrodes in hippocampal circuit for DG-LTP. (**J**) Average time course of the increase in the slope of field excitatory postsynaptic potentials (fEPSP) elicited in the DG medial molecular layer after stimulation of the MPP in hippocampal slices obtained from Ts65Dn and WT mice. (**K**) Quantification of LTP elicited in the DG of WT and Ts65Dn mice. Two-way ANOVA: genotype [$F_{1,23} = 60.530$, $P < 0.001$]; treatment [$F_{1,23} = 79.844$, $P < 0.001$], genotype x treatment [$F_{1,23} = 15.859$, $P < 0.001$]. Number in parenthesis indicates the number of samples analyzed for each experimental group. $^*P < 0.05$, $^{**}P < 0.01$, $^{***}P < 0.001$, Tukey *post hoc* test following two-way ANOVA.

proliferation deficit in trisomic adult NPCs[6,21]. However, aerobic exercise induced a 2-fold increase in the number of $BrdU^+$ cells in the DG of Ts65Dn mice and also substantially increased proliferation in WT littermates (+50%) (Fig. 2B,C). Accordingly, an immunohistochemistry analysis of the population of adult-generated newborn neurons for the early neuronal marker doublecortin (DCX)[73] showed a significant reduction in the number of DCX^+ newborn neurons in the DG of sedentary Ts65Dn mice that was completely restored to levels comparable with sedentary WT littermates following exercise (Fig. 2B–D). In addition, quantification of the long-term survival of newly generated cells and their differentiation toward the neuronal lineage using BrdU pulse-chase experiments (Fig. 2E) revealed that the number of $BrdU^+$ cells that were double-labeled with the mature neuronal marker NeuN ($BrdU^+/NeuN^+$) 4 weeks after BrdU administration was significantly reduced in sedentary Ts65Dn mice. However, the number of $BrdU^+/NeuN^+$ cells increased in both WT and Ts65Dn mice following running training (Fig. 2F,G). Moreover, the phenotypic analysis revealed that the percentage of $BrdU^+/NeuN^+$ cells among the total number of $BrdU^+$ cells was similar in all groups, indicating that the commitment toward the neuronal lineage was virtually unaffected (Fig. 2H). Based on these data, aerobic exercise efficiently restored adult neurogenesis defects in Ts65Dn mice essentially by rescuing defective NPC proliferation.

We next examined a form of long-term potentiation at medial perforant path (MPP) synapses onto dentate granule neurons (DG-LTP, Fig. 2I), which is known to depend on adult-generated newborn neurons[74–77], to assess the functional integration of adult-born neurons in Ts65Dn mice following exercise. As shown in our previous study, this *bona fide* form of neurogenesis-dependent synaptic plasticity is absent in Ts65Dn mice due to impaired adult neurogenesis and a decreased supply of newborn neurons[6]. According to previous studies, high frequency stimulation (HFS) of the MPP readily induced DG-LTP in WT slices[6,74–76], but failed to potentiate slices from Ts65Dn mice (Fig. 2J,K). Physical exercise completely restored DG-LTP in Ts65Dn mice (+19%) to levels similar to their sedentary WT littermates. Physical exercise also slightly, but significantly, increased DG-LTP in WT mice (+7%). Thus, physical exercise rescued functional adult neurogenesis in the DG of Ts65Dn mice.

Aerobic exercise rescued synaptic deficits in Ts65Dn mice. We next evaluated possible effects of exercise on non-neurogenic regions of the trisomic brain. Therefore, we first recorded spontaneous miniature excitatory and inhibitory postsynaptic currents (mEPSCs and mIPSCs, respectively) by obtaining whole-cell patch-clamp recordings from hippocampal CA1 pyramidal neurons. Miniature synaptic events (recorded in the presence of the voltage-gated sodium channel blocker TTX to prevent action potential firing) reflect the spontaneous quantal release of neurotransmitters from all presynaptic terminals converging on the recorded neuron. The frequency of these events is proportional to the total number of presynaptic terminals on the patched neuron and the probability of release at each terminal. In sedentary Ts65Dn mice, the mEPSC frequency was significantly reduced, indicating a presynaptic impairment at glutamatergic terminals. Interestingly, the mEPSC frequency was fully restored by exercise in Ts65Dn mice to a level comparable to WT mice (Fig. 3A,B). The change in the frequency was not accompanied by an alteration in the amplitude of these events, suggesting that postsynaptic glutamatergic receptors functioned normally in Ts65Dn mice. In contrast, the mIPSC frequency was similar between sedentary WT and Ts65Dn pyramidal CA1 neurons, but it was significantly reduced by running in both genotypes, without detectable changes in amplitude, consistent with previous reports[78] (Fig. 3C,D). These electrophysiological results revealed a previously unrecognized synaptic deficit that was specific for glutamatergic synapses in the trisomic CA1 field and was effectively rescued by exercise. In particular, the decrease in mEPSC frequency suggests a decrease in the number of glutamatergic synapses in Ts65Dn hippocampus. We evaluated the density of glutamatergic and GABAergic synapses in the hippocampal CA1 stratum radiatum by immunostaining for the specific presynaptic markers vGLUT1 (vesicular glutamate transporter 1) and vGAT (vesicular GABA transporter), respectively, to elucidate this hypothesis. Consistent with the observed decrease in mEPSC frequency, the density of vGLUT1-positive puncta was decreased in sedentary Ts65Dn mice, indicating a substantial paucity of glutamatergic synapses. Remarkably, aerobic exercise completely restored the density vGLUT1-positive puncta in Ts65Dn mice and significantly decreased the density of vGAT-positive puncta in both WT and Ts65Dn mice (Fig. 3E–G), indicating that exercise extensively regulated synaptogenesis. Moreover, an ultrastructural morphometric analysis using transmission electron microscopy (TEM) showed that the density of total synaptic vesicles (SVs) and the synaptic bouton area were similar in all experimental groups for both asymmetric (glutamatergic) and symmetric (GABAergic) synapses (Supplementary Fig. 3). Conversely, the length of the active zone (AZ) in asymmetric synapses was increased by exercise in both genotypes, whereas the

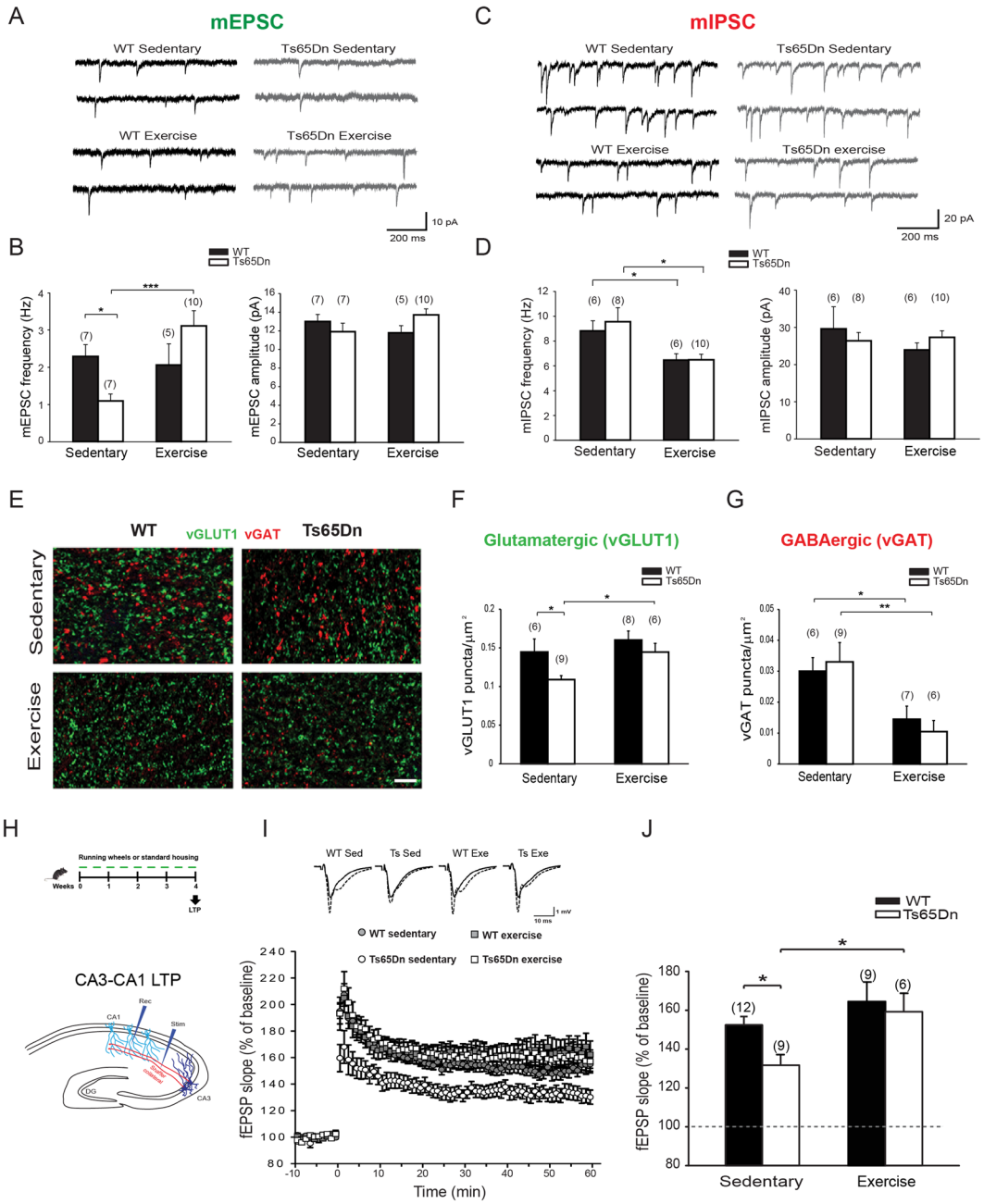

Figure 3. Physical exercises rescues synaptic deficits in Ts65Dn mice. (**A**) Representative traces showing spontaneous miniature excitatory postsynaptic currents (mEPSC) recorded from CA1 pyramidal neurons of WT and Ts65Dn mice in the presence of GABA receptors blockers. (**B**) mEPSC frequency was reduced in sedentary Ts65Dn mice and fully restored by physical exercise. Two-way ANOVA: genotype [$F_{1,25=}$0.0361, $P=0.851$]; treatment [$F_{1,25=}5.076$, $P=0.033$]; genotype x treatment [$F_{1,25}=8.018$, $P=0.009$]. mEPSCs amplitude was not significantly different across experimental groups. (**C**) Representative traces showing spontaneous miniature inhibitory postsynaptic currents (mIPSC) recorded from CA1 pyramidal neurons of WT and Ts65Dn mice in the presence of glutamate receptors blockers. (**D**) mIPSC frequency was reduced by running in both WT and Ts65Dn mice. Two-way ANOVA: [$F_{1,26}=0.0497$, $P=0.825$]; treatment [$F_{1,26}=14.628$, $P<0.001$]; genotype x treatment [$F_{1,26}=0.0348$, $P=0.854$]. mIPSC amplitude was not significantly different across experimental groups. (**E**) Representative confocal images showing VGAT (red) and VGLUT1 (green) immunostaining. Scale bars: 2 µm. (**F**) The number of VGLUT1-positive glutamatergic synapses was fully rescued by exercise in the CA1 region of Ts65Dn hippocampus. Two-way ANOVA: genotype [$F_{1,25}=5.293$, $P=0.030$]; treatment [$F_{1,25}=5.239$, $P=0.031$]; genotype x treatment [$F_{1,25}=0.806$, $P=0.378$]. (**G**) The number of VGAT-positive GABAergic synapses was decreased by exercise in the CA1 region of both Ts65Dn and WT mice. Two-way ANOVA: genotype [$F_{1,24}=1.665$, $P=0.209$]; treatment [$F_{1,24}=15.933$, $P<0.001$]; genotype x treatment [$F_{1,24}=0.328$, $P=0.572$]. (**H**) Schematic representation of the hippocampal circuit and positioning of the stimulating and recording electrodes for LTP at Shaffer collateral-CA1 synapses (CA3-CA1 LTP). (**I**) Average time course of the increase in the slope of fEPSP elicited in the CA1 Stratum Radiatum by stimulation

of the Shaffer collateral in hippocampal slices obtained from Ts65Dn and WT mice. (**J**) Quantification of CA3-CA1 LTP. Two-way ANOVA: genotype [$F_{1,32} = 3.126$, $P = 0.087$]; treatment [$F_{1,32} = 7.269$, $P = 0.011$]; genotype x treatment [$F_{1,32} = 1.109$, $P = 0.300$]. The number in parenthesis indicates the number of sample analyzed for each experimental group. *$P < 0.05$, **$P < 0.01$, ***$P < 0.001$, Tukey *post hoc* test following two-way ANOVA.

density of docked SVs in symmetric synapses was increased in Ts65Dn mice following exercise. However, these ultrastructural differences were relatively small compared to the changes observed in the density of vGLUT1- and vGAT-positive puncta (Fig. 3E–G).

Since exercise completely restored synaptic deficits in the CA1 region of trisomic animals, we next investigated whether this observation translated to a rescue of the impairment in synaptic plasticity in Ts65Dn mice. We next evaluated LTP induction elicited by theta burst stimulation (TBS) at the Schaffer collateral-CA1 pathway (CA3-CA1 LTP, Fig. 3H) to address this question, and found that potentiation was significantly lower in slices from sedentary Ts65Dn mice than in slices from WT littermates (Fig. 3I,J), similar to a previous report[20]. However, one month of physical exercise increased LTP induction at CA3-CA1 synapses in Ts65Dn mice (+28%) to levels indistinguishable from sedentary WT mice, whereas potentiation was unaltered in WT littermates ($P = 0.21$). Thus, physical exercise indeed effectively restores hippocampal synaptic plasticity in Ts65Dn mice in the CA3-CA1 circuit.

Aerobic exercise promoted BDNF expression. Aerobic exercise has been shown to increase the expression of brain-derived neurotrophic factor (BDNF) in the brain[23–25,40,41,79], and exercise-induced upregulation of BDNF has been shown to be necessary for the enhancement of adult neurogenesis and spatial memory[47,49,50]. We therefore analyzed hippocampal BDNF expression in WT and Ts65Dn mice following the exercise paradigm. According to both ELISA and immunoblot quantification, the expression of the BDNF protein was indeed similarly upregulated by exercise in WT and Ts65Dn mice (+50%) (Fig. 4A,B and Supplementary Fig. 4). BDNF mRNA transcripts are characterized by alternative exon usage at the 5′ untranslated region (UTR) and a common coding sequence (CDS). The expression of these alternative BDNF transcripts is controlled by multiple promoters that differentially contribute to activity-dependent BDNF induction[80–82]. An analysis of the expression of different BDNF transcripts by real-time quantitative PCR (RT-qPCR) revealed that the exercise-induced increase in BDNF expression was mainly due to an enhancement of transcription from exons I, II and III in both WT and Ts65Dn mice (Fig. 4C), indicating that the molecular effectors of exercise that are recruited to enhance BDNF expression are substantially spared in trisomy.

The BDNF-mimetic drug 7,8-dihydroxyflavone rescued synaptic plasticity and cognitive deficits in Ts65Dn mice. The data reported above indicate a positive correlation between increased BDNF expression and memory enhancement in Ts65Dn mice. This link is also supported by a large body of evidence showing that many of the positive effects of exercise on the brain are mediated by BDNF[40,41,44,47,49,50]. Therefore, we next investigated whether pharmacological induction of BDNF signaling in trisomic mice would be sufficient to rescue the learning and memory impairment in trisomic animals. Therefore, we took advantage of the recently developed BDNF-mimetic drug 7,8-dihydroxyflavone (DHF), which crosses the brain-blood barrier upon oral administration[83] and induces BDNF/TrkB signaling[84–95]. Previous reports have shown that acute DHF administration (5 mg/kg body weight) was able to promote TrkB phosphorylation in the brain; yet one study could not detect such effect[84,86,92]. Therefore, we assessed the levels of TrkB phosphorylation after acute DHF administration at the same dose. However, we could not detect any increase in the level of phosphorylated TrkB at Tyr817 (P-TrkB^{Tyr817}) in either the hippocampus or cortex of both WT and Ts65Dn mice 1 hour after DHF administration (Fig. 5A,B). Nonetheless, other studies have reported activation of TrkB after chronic DHF treatment[87,90–95]. Accordingly, we found that chronic (4 weeks) administration of DHF significantly increased the level of P-TrkB^{Tyr817} (+26%) in the hippocampus of Ts65Dn mice (Fig. 5C). Notably, DHF-induced TrkB phosphorylation only showed a small increasing trend in the hippocampus of WT animals, but it did not reach statistical significance ($P = 0.091$). Still, in the same group of WT and Ts65Dn animals, we could not detect a significant increase of P-TrkB^{Tyr817} in the cortex (Fig. 5D).

Next, we evaluated whether the chronic DHF treatment rescued hippocampal synaptic plasticity in Ts65Dn mice. The chronic DHF treatment largely phenocopied the effect of exercise on Ts65Dn mice by increasing CA3-CA1 LTP (+23%) to levels similar to vehicle-treated WT animals (Fig. 5E–G). Interestingly, the DHF treatment also increased CA3-CA1 LTP in WT mice (+17%), highlighting the well-known involvement of TrkB signaling in synaptic plasticity[53–55].

Furthermore, we evaluated whether the rescue of hippocampal synaptic plasticity induced by the DHF treatment was paralleled by a recovery of cognitive deficits in trisomic animals. Chronic DHF treatment was well tolerated by mice and it did not induce changes in body weight gain or motor activity in either WT or Ts65Dn mice (Supplementary Fig. 5). The DHF treatment indeed rescued associative learning in DS mice in the CFC test, similar to the rescue observed with aerobic exercise (Fig. 6A,B), without inducing changes in non-associative freezing or altering sensitivity to the shock (Supplementary Fig. 6A). Moreover, spatial and discriminative memories were rescued by DHF in the OL and NOR tests (Fig. 6C,D), independent of object preference (Supplementary Fig. 6B,C). In contrast to aerobic exercise and the effects of the DHF treatment on T65Dn mice, DHF did not show a statistically significant effect on WT mice. Based on these data, the DHF treatment rescues different forms of memory in Ts65Dn mice. These data also point to the substantial specificity of the beneficial effect of strategies promoting BDNF/TrkB signaling on DS mice.

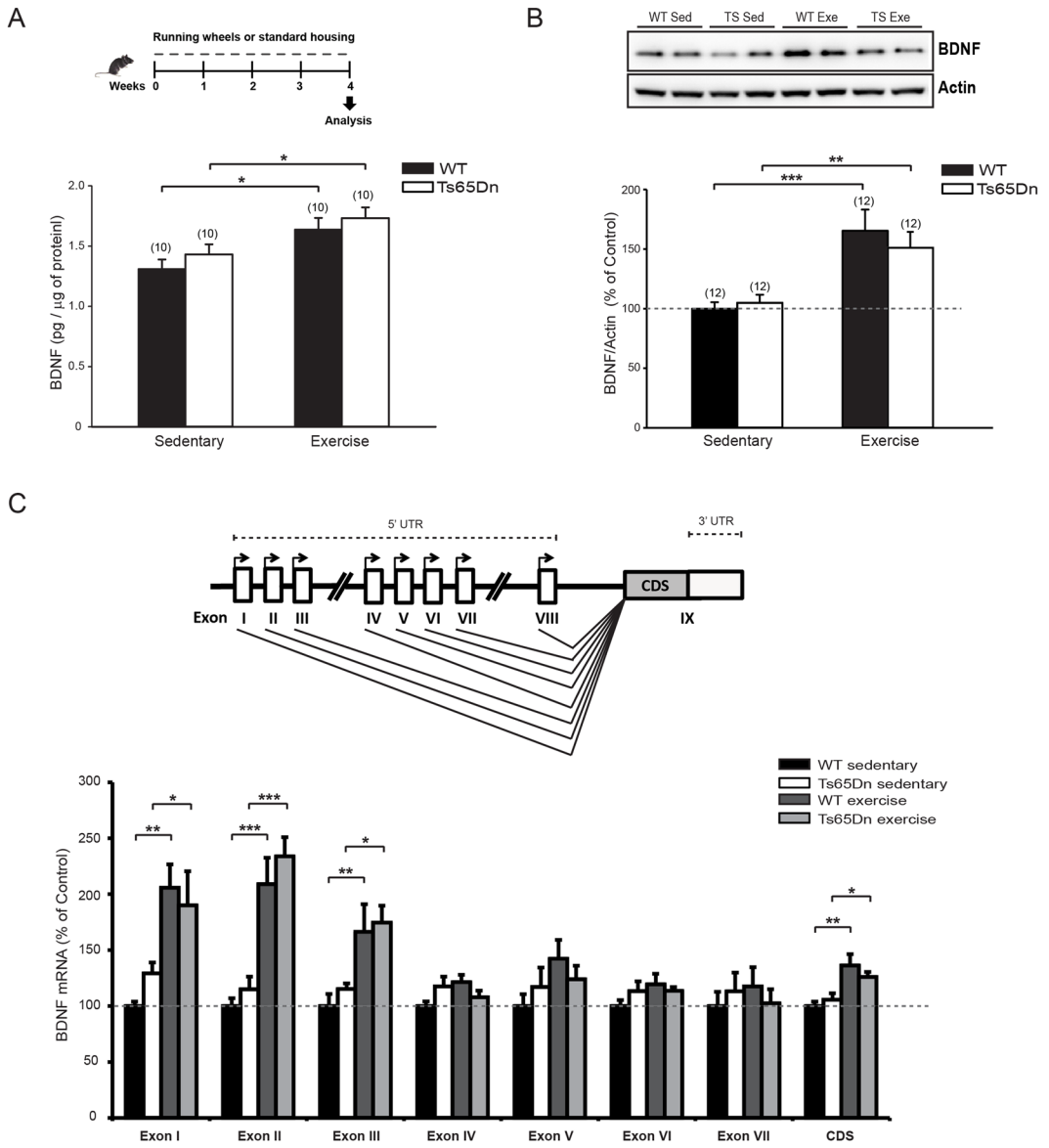

Figure 4. Physical exercise increased BDNF expression in the hippocampus of mice. (**A**) *Top*, schematic representation of the experimental protocol. *Bottom*, quantification of BDNF expression by ELISA immunoassay showed increased expression in the both WT and Ts65Dn running groups. Two-way ANOVA: genotype [$F_{1,36} = 1.534$, $P = 0.224$]; treatment [$F_{1,36} = 12.862$, $P < 0.001$]; genotype x treatment [$F_{1,36} = 0.0224$, $P = 0.882$]. (**B**) *Top*, representative immunoblot for BDNF in protein extracts from hippocampal samples collected from Ts65Dn and WT mice. *Bottom*, quantification of BDNF (expressed as percentage of sedentary WT) showed increased expression following exercise in the both WT and Ts65Dn mice. Actin was used an internal standard. Two-way ANOVA on ranked-transformed data: genotype [$F_{1,44} = 0.000$, $P = 1.000$]; treatment [$F_{1,44} = 27.322$, $P < 0.001$]; genotype x treatment [$F_{1,44} = 0.547$, $P = 0.464$]. The numbers in parenthesis indicates the number of samples for each experimental group. (**C**) *Top*, schematic representation of mouse *Bdnf* gene showing the exon organization of the 5′ and 3′ untranslated regions (UTR; white) and coding sequence (CDS; grey). *Bottom*, RT-qPCR analysis of mouse BDNF mRNA (expressed as percentage of sedentary WT) showed increased expression of transcripts from exons I, II, III and CDS in the hippocampus of exercised mice (n = 5-6 for each experimental group). $^{*}P < 0.01$, $^{**}P < 0.01$, $^{***}P < 0.001$, Tukey *post hoc* test following two-way ANOVA. Full-length blots are presented in Supplementary Fig. 7.

BDNF expression is decreased in the brains of patients with DS. We next evaluated BDNF expression in the hippocampus of adult patients with DS (13–39 years old) prior to the development of an obvious Alzheimer's neuropathology to obtain insights into the possible translational applicability of a BDNF-mimetic strategy as a treatment for cognitive impairment. Interestingly, BDNF expression was substantially reduced at both the mRNA and protein levels in the hippocampus of patients with DS compared to age/gender-matched normal controls (Fig. 7A,B), indicating that BDNF/TrkB signaling is likely defective in individuals with DS. As shown it the scatter plot representation of BDNF protein and mRNA expression, although the control and DS

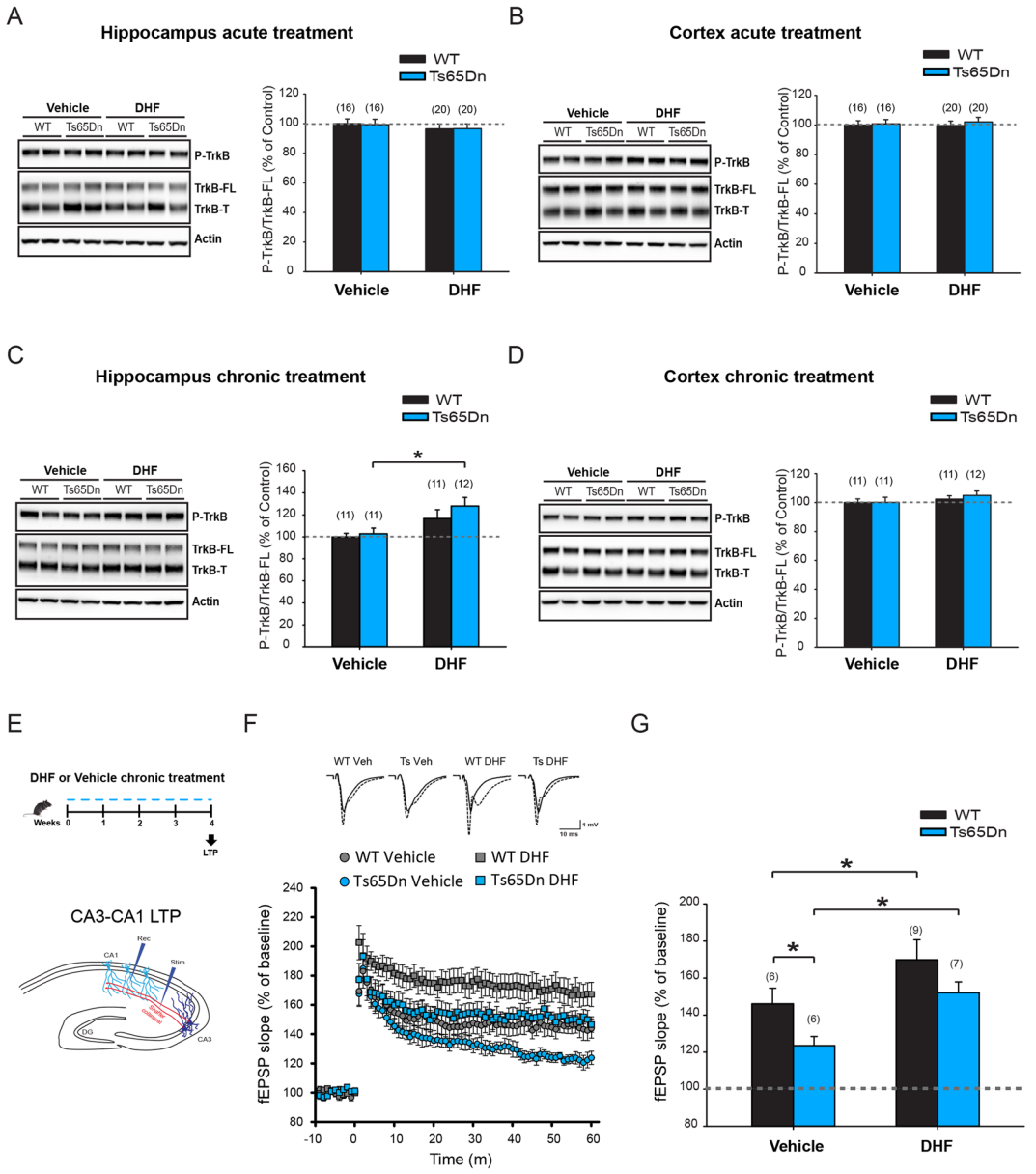

Figure 5. The BDNF-mimetic drug DHF stimulated TrkB signaling and rescued synaptic plasticity deficits in the hippocampus of Ts65Dn mice. (**A**) *Left*, representative immunoblot for phosphorylated (Tyr817) or total TrkB (full-length and truncated isoforms: FL and T, respectively) and Actin in protein extracts from hippocampal samples collected from Ts65Dn and WT mice 1 hour after acute administration of DHF (5 mg/kg) or vehicle. *Right*, quantification of P-TrkB^{Tyr817} (expressed as percentage of vehicle-treated WT) did not show differences after acute DHF administration. Two-way ANOVA on ranked-transformed data: genotype [$F_{1,68} = 0.099$, $P = 0.753$]; treatment [$F_{1,68} = 1.730$, $P = 0.193$]; genotype x treatment [$F_{1,68} = 0.061$, $P = 0.806$]. (**B**) *Left*, representative immunoblot for phosphorylated or total TrkB and Actin in protein extracts from cortical samples collected from Ts65Dn and WT mice 1 hour after acute administration of DHF or vehicle. *Right*, quantification of P-TrkB^{Tyr817} did not show differences after acute DHF administration. Two-way ANOVA: genotype [$F_{1,68} = 0.315$, $P = 0.576$]; treatment [$F_{1,68} = 0.019$, $P = 0.892$]; genotype x treatment [$F_{1,68} = 0.081$, $P = 0.776$]. (**C**) *Left*, representative immunoblot for phosphorylated or total TrkB and Actin in protein extracts from hippocampal samples collected from Ts65Dn and WT mice chronically treated for 4 weeks with DHF or vehicle. *Right*, quantification of P-TrkB^{Tyr817} showed a significant increase in the hippocampus of DHF-treated Ts65Dn mice. Two-way ANOVA on ranked-transformed data: genotype [$F_{1,41} = 2.383$, $P = 0.130$]; treatment [$F_{1,41} = 9.135$, $P = 0.004$]; genotype x treatment [$F_{1,41} = 0.302$, $P = 0.586$]. (**D**) *Left*, representative immunoblot for phosphorylated or total TrkB and Actin in protein extracts from cortical samples collected from Ts65Dn and WT mice chronically treated for 4 weeks with DHF or vehicle. *Right*, quantification of P-TrkB^{Tyr817} did not show differences in the cortex of Ts65Dn and WT mice. Two-way ANOVA: genotype [$F_{1,41} = 0.203$, $P = 0.665$]; treatment [$F_{1,41} = 1.570$, $P = 0.217$]; genotype x treatment [$F_{1,41} = 0.116$, $P = 0.686$]. (**E**) Schematic representation of the experimental protocol and positioning of the stimulating and recording electrodes in hippocampal circuit for LTP at Shaffer collateral-CA1 synapses. (**F**) Average time course of the increase in the

slope of fEPSP elicited in the CA1 Stratum Radiatum by stimulation of the Shaffer collateral in hippocampal slices obtained from Ts65Dn and WT mice. (**G**) Quantification of CA3-CA1 LTP. Two-way ANOVA: genotype [$F_{1,24} = 8.459$, $P = 0.008$]; treatment [$F_{1,24} = 13.530$, $P = 0.001$]; genotype x treatment [$F_{1,24} = 0.0593$, $P = 0.810$]. The number in parenthesis indicates the number of sample analyzed for each experimental group. *$P < 0.05$, Tukey *post hoc* test following two-way ANOVA. Full-length blots are presented in Supplementary Fig. 7.

groups were clearly separated (Fig. 7C), the correlation between mRNA and protein levels in individual samples was relatively low (Pearson's correlation coefficients: −0.09 and −0.20 for controls and patients with DS, respectively), indicating a possible dissociation between mRNA and protein levels in post-mortem human samples. However, as baseline BDNF expression is substantially downregulated at both the mRNA and protein levels in the hippocampus of patients with DS, the downstream TrkB signaling pathway is also likely to be compromised in patients with DS, thus highlighting the translational significance of developing a BDNF-mimetic strategy for the treatment of the disease.

Discussion

Significant cognitive dysfunction is nearly universal across the life span in persons with DS[2,96–101]. Although these cognitive difficulties possibly arise from dysfunction of the hippocampal circuit[2,4,102–105], we have only recently started to shed light on the neurobiological bases of these abnormalities through the use of mouse models of DS[6,11,13–15,17–20,66,78,106,107]. However, little progress has been achieved in translating these findings into clinically effective treatments to date.

Here, the use of either aerobic exercise or a pharmacological treatment to promote BDNF signaling rescues cognitive symptoms in DS mice. Indeed, according to studies of human subjects and animal models, aerobic physical exercise induces BDNF expression, which, in turn, promotes structural and functional plasticity of neurons, impacting on cognition and resistance to injury and diseases[22–24].

Using light weight running apparatus with reduced friction that allowed mice to run considerable distances each day, aerobic exercise rescued excitatory synaptic deficits in the hippocampal CA1 region of Ts65Dn mice by promoting functional synaptogenesis of glutamatergic terminals. This effect was paralleled by a substantial recovery of synaptic plasticity in trisomic mice, as revealed by the rescue of defective LTP at Schaffer collateral-CA1 synapses. Accordingly, previous studies have indicated a prominent role for BDNF signaling in regulating synapse formation and LTP induction[108].

According to several epidemiological studies involving children and adults, physical activity may improve cognitive performance and slow the progression of intellectual decline in aging humans[24–28,32,34–37]. In healthy humans, the levels of aerobic exercise correlate with sustained cerebral blood flow, improved memory performances, increased circulating BDNF levels and increased hippocampal grey matter volume, likely due to the promotion of adult neurogenesis in the DG[29–33,39]. Similarly, in rodents, exercise enhances hippocampus-dependent memory in different behavioral tasks[38]. The beneficial effects of aerobic exercise on rodents have also been associated with an upregulation of the BDNF/TrkB pathway[23–25,40,41], increased neurogenesis in the hippocampal DG[24,42–46], and the potentiation of synaptic plasticity[47,48].

Here, we show an aerobic exercise-induced improvement in learning and memory in different behavioral tasks in DS mice. In particular, we observed a significant improvement in different cognitive domains, including spatial memory (OL test), associative learning (CFC test) and episodic memory (NOR test). Previous studies evaluating the effect of exercise on learning and memory in DS mice have only reported limited efficacy. In the first study, exercise only partially increased spatial acquisition in the Morris water maze (MWM) in relatively old male Ts65Dn mice (aged 10–12 months), but no improvement was detected during the MWM probe trial or in DG adult neurogenesis[109]. A second study did not observe a significant impairment in sedentary female Ts65Dn mice compared to WT mice in the NOR test (but the authors used a different protocol than the protocol we used here). However, a slight increase in preference for the novel object was observed in Ts65Dn females when the mice were allowed access to running wheels beginning at weaning, but not when the exercise paradigm was administered in adulthood (starting from 7 to 17 months of age)[110]. Compared to our strong positive results, one main reason for the previously reported negative outcomes may reside in the low amount of running performed by aged Ts65Dn mice. Similarly, different behavioral tasks used for evaluations of cognitive performances and age- and gender-related differences in the animals may also contributed to the difference between our positive results and previous findings.

Based on our results, the recovery of normal levels of cognitive function was accompanied by both structural and functional rescue of different deficits in the trisomic brains. Consistent with previous studies highlighting the neurogenic effect of aerobic exercise[46,48], voluntary wheel-running rescued adult neurogenesis in the hippocampal DG of Ts65Dn mice in our study. In particular, wheel-running rescued impaired NPC proliferation and substantially increased the number of newly generated neurons in the DG of Ts65Dn mice. Importantly, the recovery of adult DG neurogenesis was paralleled by the functional integration of the newly generated neurons in the hippocampal circuit, since a *bona fide* form of neurogenesis-dependent dentate LTP[74–77], which is absent in Ts65Dn mice[6], was in fact completely rescued by exercise. Consistent with previous studies[46,48,68], wheel running increased hippocampal adult neurogenesis, DG-LTP and improved cognitive performances in WT mice; these effects where somewhat milder than in trisomic animals. Previous studies have reported a positive correlation between DG adult neurogenesis and cognitive performances in Ts65Dn mice[6,111,112], highlighting the important role of this form of structural plasticity in the brain on neurophysiology and learning deficits in trisomic animals.

We were also interested in identifying possible effects of exercise that were specific for trisomic animals and occurred in addition to DG adult neurogenesis. Accordingly, we report here for the first time that the frequency

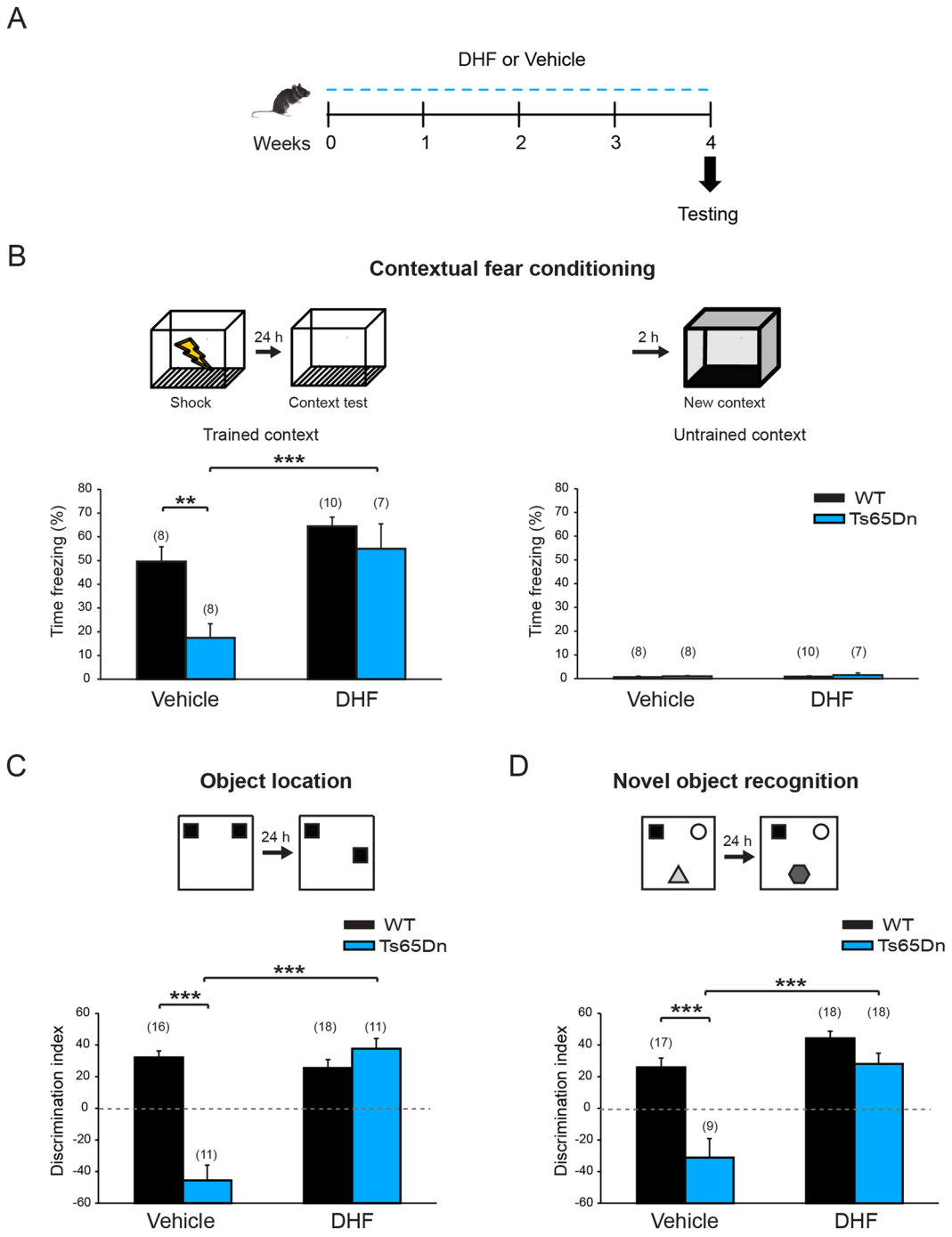

Figure 6. DHF treatment rescued memory deficits in Ts65Dn mice. (**A**) Schematic representation of the experimental protocol. (**B**) *Top*, schematic representation of the contextual fear conditioning test. *Left*, one month of DHF treatment rescued contextual memory in Ts65Dn mice. Two-way ANOVA: genotype [$F_{1,29} = 9.920$, $P = 0.004$]; treatment [$F_{1,29} = 15.754$, $P < 0.001$]; genotype x treatment [$F_{1,29} = 2.959$, $P = 0.096$]. *Right*, both WT and Ts65Dn mice showed negligible freezing response when exposed to a new context. (**C**) Schematic representation of the object location (OL) test. Ts65Dn mice showed an absolute inability to discriminate the new object location after a retention interval of 24 hours. DHF restored spatial memory in Ts65Dn mice. Two-way ANOVA: genotype [$F_{1,52} = 26.522$, $P < 0.001$]; treatment [$F_{1,52} = 36.311$, $P < 0.001$]; genotype x treatment [$F_{1,52} = 49.978$, $P < 0.001$]. (**D**) Schematic representation of the novel object recognition (NOR) test. One month of DHF treatment rescued novelty discrimination deficits in Ts65Dn mice in the NOR test. Two-way ANOVA: genotype [$F_{1,58} = 27.343$; $P < 0.001$]; treatment [$F_{1,58} = 32.390$; $P < 0.001$]; genotype x treatment [$F_{1,58} = 9.182$; $P = 0.004$]. For all panels the number in parenthesis indicates the number of mice tested for each experimental group. $^{*}P < 0.05$, $^{**}P < 0.01$, $^{***}P < 0.001$, Tukey *post hoc* test following two-way ANOVA.

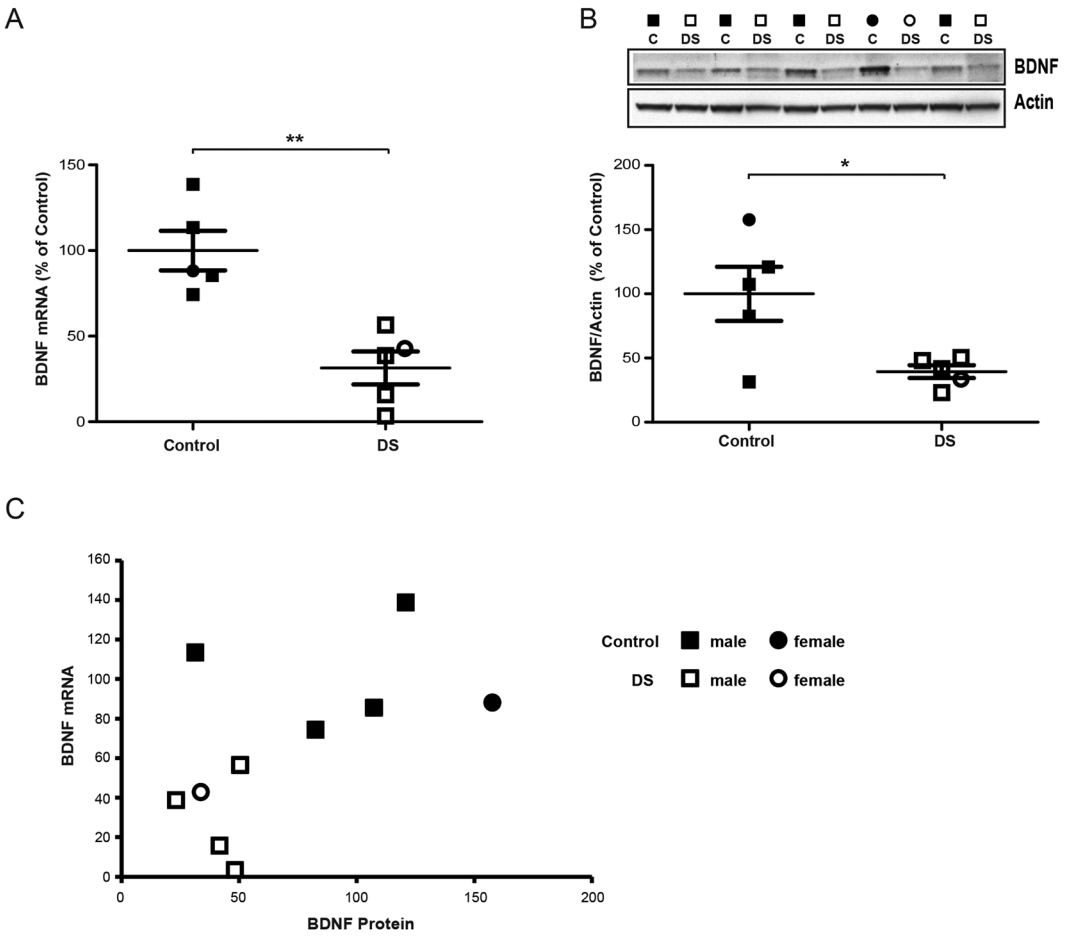

Figure 7. BDNF expression is reduced in the hippocampus DS patients. (**A**) RT-qPCR quantification of BDNF mRNA in the hippocampus of adult DS patients (open symbols: □ males; ○ females) in comparison to age/sex matched non-trisomic controls (solid symbols: ■ males; ● females). Group averages (±SEM) are reported by lines. (**B**) *Top*, representative immunoblot for BDNF in protein extracts from human post-mortem whole hippocampus (gender is indicated above as squares for males and circles for females). *Bottom*, quantification of BDNF (expressed as percentage of controls) showed decreased expression in the hippocampus of adult DS patients in comparison to age/sex matched non-trisomic controls. Actin was used an internal standard. (**C**) Scatterplot representation of BDNF protein and mRNA expression for each individual samples. $*P < 0.05$, $**P < 0.01$ unpaired Student's t-test. Full-length blots are presented in Supplementary Fig. 7.

of mEPSCs recorded from CA1 pyramidal neurons (*i.e.*, a non-neurogenic hippocampal region) was decreased in sedentary Ts65Dn mice compared to WT mice and was effectively restored by exercise. Notably, the density of glutamatergic synapses in hippocampal stratum radiatum was also reduced in sedentary Ts65Dn mice and rescued by exercise. These results are consistent with previous immunohistochemical and electron microscopic studies showing a general decrease in the glutamatergic synapse density in the brains of Ts65Dn mice[17,107,113–117] along with a decrease in the mEPSC frequency in the hippocampal CA3 field[12,17]. Although the effect of exercise on mEPSC frequency and glutamatergic synapse density appeared to be specific for trisomic brains in the present study, exercise also significantly reduced the density of GABAergic synapses and mIPSC frequency in both WT and Ts65Dn mice. We cannot exclude the possibility that the difference in miniature postsynaptic current frequency may at least partially depend on changes in release probability, but the data presented here generally support the conclusion that variations in the number of glutamatergic and GABAergic synapses, rather than alterations in the SV pools[118,119], are linked to changes in both mEPSC and mIPSC frequencies. Consistent with our data, the density of GABAergic terminals in the brains of Ts65Dn mice was similar to WT mice in previous studies[14,114,115,120,121]. Furthermore, according to previous electrophysiological analyses, the mIPSC frequency, release probability at GABAergic synapses and $GABA_A$-mediated transmission were unaffected in the hippocampal CA1 region of Ts65Dn mice[13,78]. However, possible sub-regional differences may exist in the trisomic hippocampus, since other studies have observed an increased GABAergic synapse density in the inner molecular layer of the DG in Ts65Dn mice[19,117]. This finding was supported by the observation that the mIPSC frequency and evoked GABAergic transmission were increased in the DG of Ts65Dn mice[11,14]. The potential occurrence of sub-regional differences in GABAergic innervation was also further highlighted by the observation that the mIPSC frequency was actually decreased in CA3 region of the Ts65Dn hippocampus[12,17]. Most importantly, Ts65Dn synaptic

plasticity deficits and cognitive impairments were suggested to arise from an imbalance between excitatory and inhibitory neurotransmission[10–16]. Based on our results, running-mediated recovery of the excitatory/inhibitor balance was paralleled by the selective rescue of LTP at CA3-CA1 synapses in exercised Ts65Dn mice. Consistent with previous studies, we did not observe significant differences in CA3-CA1-LTP between sedentary and running WT animals[48], although exercise-induced changes in the GABAergic synapse density and mIPSC frequency (but not glutamatergic synapse density and mEPSC frequency) were similar to the changes observed in Ts65Dn littermates. Therefore, the dual effects of physical exercise on both glutamatergic and GABAergic synapses in Ts65Dn mice likely contributes to the observed rescue of synaptic plasticity and cognitive performance.

Similar to aerobic exercise, environmental enrichment (EE) also represents a non-pharmacological method to promote brain plasticity, adult neurogenesis, BDNF expression and learning[71,122,123]. Indeed, previous studies on Ts65Dn mice exposed to EE have shown a substantial recovery of synaptic plasticity and cognitive performances, as well as increased BDNF expression and reduced neurotransmitter release from GABAergic terminals[65,124]. In this regard, enriched cages were also equipped with running wheels in these experiments; therefore, some of the beneficial effects of EE may actually be ascribed to exercise. Interestingly, exercise has recently been shown to be a key factor that mediates increased BDNF expression, adult neurogenesis and enhanced cognitive performances in response to EE[68,79,125]. Our results showing a reduced density of vGAT-positive puncta and mIPSC frequency in both WT and Ts65Dn mice after running clearly suggest that exercise is an active component of the ability of the EE paradigm to modulate GABAergic functions. Interestingly, a study of Ts65Dn mice[126] has suggested EE as a complementary adjuvant to pharmacological therapy with a polyphenolic green tea extract enriched in epigallocatechin-3-gallate (EGCG). Similarly, a recent clinical trial in patients with DS has introduced a computer-based cognitive training paradigm as an adjuvant to a green tea extract treatment[127]. Some encouraging, although limited, reports have indicated that aerobic exercise may be beneficial in improving executive functions in patients with DS[128–130]. Therefore, a controlled exercise paradigm may also be a valuable complementary intervention to pharmacological therapies for patients with DS. Nevertheless, in our experimental setting, animals ran a considerable distance each day, and Ts65Dn mice ran an even greater distance. The increased activity observed in trisomic animals may likely be attributed to the reported hyperactivity of this mouse model[5]. However, from the clinical perspective, when considering the large distance travelled daily by Ts65Dn mice in our experiments, exercise may not be a practical medical intervention, since it strongly depends on motivation, which may be low in individuals with DS. Thus, a pharmacological approach, such as the one we propose here with DHF, mimicking the molecular changes induced by aerobic exercise may be an alternative and valuable therapeutic intervention.

BDNF has been postulated to act as a key mediator of exercise-associated cognitive improvement, enhanced neurogenesis and synaptic plasticity[23,40,44,47,49,50,68]. Similar to previous reports[17,65–67,131,132], we confirm here that basal hippocampal BDNF levels are similar in young and middle-aged Ts65Dn mice compared to WT mice. However, BDNF expression was reduced in CA1 hippocampal neurons of elderly Ts65Dn mice[133], indicating an age-related impairment in BDNF expression in trisomic mice. In this regard, some conflicting results have been reported in the literature, since BDNF expression was reduced in the hippocampus of both young and middle-aged Ts65Dn mice[134–137]. As BDNF expression is influenced by previous experience, gender, circadian rhythms or housing conditions[138–142], differences in these variables and the analysis method used may explain the reported discrepancies. Additionally, BDNF levels are reduced in the hippocampal DG (but not CA1) and frontal and visual cortices of Ts65Dn mice[65,131], indicating that regional and sub-regional differences in neurotrophin expression may occur in trisomic animals. On the other hand, BDNF expression was previously reported to be decreased in lymphoblastoid cell lines from individuals with DS[143]. Accordingly, we provide new evidence in this study showing that BDNF levels are substantially reduced in the hippocampus of young adults (mean age 23 years) with DS, indicating that in contrast to animal models, the BDNF deficiency occurs earlier in persons with DS. Therefore, a BDNF-mimetic pharmacological intervention in individuals with DS may represent a strong therapeutic opportunity to rescue cognitive disabilities. Based on the known pivotal effect of BDNF signaling on cognition[108,144], the observed increase in BDNF expression in Ts65Dn mice compared to the basal level may contribute to the beneficial effect of running we observed in these mice. This result is consistent with other studies showing that the recovery of normal levels of cognitive function in Ts65Dn mice induced by different pharmacological interventions or EE are paralleled by increased BDNF expression[17,65–67]. Nevertheless, the BDNF level *per se* does not completely account for its downstream effects, since the neurotrophin is actively released at synapses and acts at both pre- and post-synaptic sites to regulate several processes through different intracellular signaling cascades[108,145–147]. Indeed, a recent study reported reduced surface binding of BDNF-conjugated Quantum dots (QD-BDNF) to Ts65Dn cortical synaptosomes compared to WT synaptosomes, together with a severely blunted response of the phosphorylation cascade downstream of TrkB upon BDNF application[148], indicating that synaptic BDNF/TrkB signaling is likely altered in Ts65Dn mice.

Experiments assessing whether strategies that increase BDNF signaling compared to its basal level may be sufficient to rescue the cognitive impairment in Ts65Dn mice are worthwhile in view of the possible translation to patients with DS. We therefore searched for a possible pharmacological treatment that mimicked the effect of physical exercise on potentiating BDNF signaling. We tested the effect of the BDNF-mimetic drug DHF that is orally active, crosses the brain-blood barrier, promotes TrkB phosphorylation and has been proven to be safe and well tolerated in rodents and primates[84–95,149–151]. Moreover, according to the results from *in vivo* pharmacokinetic studies in mice, DHF efficiently penetrates the brain after oral administration (50 mg/Kg), showing a brain to plasma concentration ratio of approximately 1:1 and an elimination half-life of about 2 hours[83]. However, an even longer half-life of 4–8 hours was measured in primate plasma after oral administration (30 mg/Kg)[150]. Although DHF has been shown to activate TrkB in the brain after acute administration[85,86], we failed to detect any increase in TrkB phosphorylation in both WT and Ts65Dn mice after a single dose. Such discrepancy may at least partially arise from difference in the brain area analyzed in previous studies. However, our results are consistent with at

least one report showing increased TrkB phosphorylation only after chronic, but not acute DHF treatment in the hippocampus of the Tg2576 mouse model of Alzheimer's disease[92]. In keeping with this and other reports[87,90–95], we found that chronic DHF treatment increased TrkB phosphorylation in the hippocampus of Ts65Dn mice. However, we could not find a statistically significant increase in TrkB phosphorylation in the hippocampus of their WT littermates. This result may indicate increased sensitivity to the drug in DS mice compared to WT, a hypothesis supported by previous observations showing increased TrkB phosphorylation in different mouse brain disease models, but not in the corresponding control animals[88,92,94]. Interestingly, the effect of DHF on TrkB phosphorylation was possibly specific for the hippocampus because the level of P-TrkB^{Tyr817} was similar in the cortex of DHF- and vehicle-treated Ts65Dn mice. This indicates a possible different sensitivity to the drug in the cortex or the occurrence of compensatory and/or desensitization mechanisms.

Chronic oral administration of DHF rescued hippocampal synaptic plasticity and cognitive function in Ts65Dn mice. These results largely mimicked the effect of exercise on Ts65Dn mice. However, the DHF treatment enhanced hippocampal synaptic plasticity in WT to similar levels as trisomic animals, but it was unable to promote learning and memory in WT mice. Therefore, in contrast to physical exercise, the DHF treatment appeared to specifically enhance cognitive functions in trisomic animals, but not in WT littermates. Although we have not investigated this aspect, one possible explanation may be that overstimulation of this pathway in animals with intact BDNF signaling, as presumably found in WT mice, will have little effect on cognition. This possibility is corroborated by previous studies showing a positive effect of DHF on learning and memory in cognitively impaired animals, but not in the corresponding WT[89,152]. Alternatively, aerobic exercise may also recruit other signaling pathways relevant for memory in addition to BDNF in WT animals. However, in trisomic animals, where multiple neuronal and synaptic functions (possibly including neurotrophin signaling) are compromised, the stimulation of BDNF signaling may be sufficient to rescue cognitive functions.

Moreover, the effect of DHF appeared to be consistent with previous studies showing that the administration of Neurotropin® (a drug previously proposed as analgesic for chronic pain) or ciliary neurotrophic factor (CNTF) peptide to increase hippocampal BDNF expression in Ts65Dn mice is associated improved spatial memory[134,137]. Regarding translational opportunities afforded by the present results, physical exercise may represent a valuable complementary therapy aimed at rescuing cognitive disabilities in patients with DS.

Although the care of associated medical issue has largely improved the overall health and life expectancy of individuals with DS, no effective pharmacological treatment is currently available to rescue cognitive deficits. Here, we report pre-clinical data on this widely used mouse model of DS showing that either aerobic physical exercise and/or a DHF pharmacological treatment may represent a promising intervention for alleviating the learning and memory deficits of patients with this syndrome.

Material and Methods

Animals and treatment. Ts65Dn colony[5] was maintained by crossing Ts65Dn female to C57BL/6JEi x C3SnHeSnJ (B6EiC3) F1 males (Jackson Laboratories; Bar Harbor, USA). Animals were genotyped by PCR as previously described[8]. Ts65Dn male mice aged between 16 and 20 weeks were used for experiments and wild-type (WT) littermates were used as controls throughout the study. Ts65Dn and WT littermates were randomly assigned to the running or sedentary groups. Running animals (two mice/cage) were housed for 4 weeks with two light weight and reduced friction running wheels (Med Associated). Sedentary mice were housed in standard cages without running wheels. For the assessment of the mean running distance, a cohort of WT and Ts65Dn mice was individually housed for 4 weeks with one running wheel equipped with a wireless revolution counting system (Med Associated). For neuron birth dating in neurogenesis experiments, mice were administrated with 5-Bromo-2-Deoxyuridine (BrdU; 100 mg/kg body weight) through daily i.p. injections, for 6 consecutive days and perfused for immunohistochemistry 24 hours or 4 weeks after the last injection[6,153].

For neurogenesis assessment and quantification of synapses density (vGAT/vGLUT1, see below), we used mice after concluding behavioral assessment in the NOR or OL test. Due to the more stressful nature of the CFC test, none of the mice subjected to this test was later used for other experiments. Detailed list of mice used in the study is provided in Supplementary Table 4.

For 7,8-dihydroxyflavone (DHF) treatment, the drug was administered through the drinking water, as previously described[149]. DHF (TCI Europe) stock solution was prepared at 100 mg/ml in dimethylsolfoxide (DMSO) and stored in aliquots at −20 °C. This stock solution was diluted at 80 mg/L in drinking water containing 0.2% (w/v) sucrose[149]. The DHF drinking solution was replaced every 2-3 days and water intake monitored throughout the experiments. The average water intake during the four weeks of treatment was used to calculate the average DHF dose received by mice, which was estimated in 22.16 ± 1.64 mg/Day/Kg body weight. Vehicle-treated mice received drinking water containing 0.08% (v/v) DMSO and 0.2% (w/v) sucrose. Chronic DHF treatment appeared to be well tolerated by mice. Only 1 out of 85 vehicle-treated mice and 1 out of 97 DHF-treated mice died during the study.

For acute drug administration, mice were treated as previously described[84,86,92] with DHF (i.p., 5 mg/Kg body weight) or the corresponding vehicle (10% DMSO in saline) and sacrificed 1 hour later. To minimize possible circadian effects on gene expression, collection of all samples for biochemical analysis was performed between 9.00 and 12.00 AM. Brains were rapidly dissected in ice-cold PBS and immediately snap-frozen.

Behavioral testing. Behavioral tests were performed on each animal during the 4th week of treatment as previously described[6,15]. Animal behavior was video-recorded throughout the experimental sessions, and subsequently analyzed by a trained operator blind to the experimental groups. WT and Ts65Dn mice were always evaluated in parallel and with the same time schedule. In order to avoid any confounding effect, tests were administrated only once to individual mice and, various cohorts of mice were used for different behavioral testing. Three days before starting the behavioral experiments mice where handled once a day for 5 min each.

Object location test (OL). This test measures spatial memory by evaluating the ability of mice to recognize the new location of familiar object with respect spatial external cues. The test was conducted in a grey acrylic arena (44 × 44 cm) equipped with a digital video recording system. The test was conducted during 3 consecutive days. On the first day mice were first habituated to the empty arena for 15 minutes. The next day the mice were exposed to 2 identical objects for 15 minutes (acquisition session). Object preference was evaluated during this session. On the third day (trial session) one the object was moved to a novel location, and the mice were allowed to explore the objects for 15 minutes. The object and the arena were cleaned with 70% ethanol after each trial. Exploratory behavior of the objects was defined as direct contact with the object by the animal mouth, nose or paws, or if the animal's nose was within 1 cm of an object (sniffing); any indirect or accidental contact with the objects was not included in the scoring. A discrimination index was calculated as the percentage of time spent investigating the object in the new location minus the percentage of time spent investigating the object in the old location: Discrimination Index = (New OL Exploration Time/Total Exploration Time * 100) − (Old OL exploration time/Total Exploration Time * 100).

Novel object location test (NOR). This test measures the preference of mice for a novel object versus previously encountered familiar objects. The test was conducted in a grey acrylic arenas (44 × 44 cm) equipped with a digital video recording system as above. The NOR test was conducted during 3 consecutive days, similarly to the OL test. On the first day the mice were habituated to the apparatus by freely exploring the empty arena for 15 minutes. The next day (acquisition session), three different objects were placed into the arena and the mice were allowed to explore for 15 minutes. Object preference was evaluated during these sessions. The objects used during the test were different in shape, color, size and material. On the third day (trial session) one the object used during the acquisition session was replaced by a novel object and the mice were allowed to freely explore the objects for 15 minutes. The objects and the arena were cleaned with 70% ethanol between trials. Exploratory behavior of the object was defined as direct contact with the object by the animal mouth, nose or paws, or if the animal's nose was within 1 cm of an object (sniffing); any indirect or accidental contact with the objects was not included in the scoring. A discrimination index was calculated as the difference between the percentages of time spent investigating the novel object and the time spent investigating the familiar objects: Discrimination Index = (New Object Exploration Time/Total Exploration Time * 100) − (Familiar Object Exploration Time/Total Exploration Time * 100).

Motor activity. The distance traveled by mice in the empty arena during the habituation sessions of the OL and NOR tests was measured with ANY-maze tracking software (Stoelting).

Contextual fear conditioning test (CFC). The fear conditioning system (TSE) consisted of a transparent acrylic conditioning chamber (20 × 10 cm) equipped with a stainless-steel grid floor and a digital video recording system. Mice were held outside the experimental room in their home cages prior to testing and individually transported to the conditioning apparatus in standard cages. The mice were placed in the conditioning chamber and 3 minutes later, received one electric shock (2 s, 0.75 mA constant electric current) through the floor grid. Mice were removed 15 s follow the shock. 24 hours later, the mice were placed in the same chamber for 3 minutes (context test) and after 2 hours moved to a new context (black chamber with plastic gray floor and vanilla odor). The chamber was cleaned with 70% ethanol after each trial. The freezing behavior was scored by a trained operator blinded to the experimental groups.

The NOR and OL test were performed in dim light illumination (12–14 Lux), while CFC was conducted with standard illumination (80 Lux). In behavioral experiments, we adopted the following exclusion criteria independently of genotype or treatment (before blind code break). In the CFC test, we excluded mice showing very high non-associative freezing in the new context: more than 30 seconds freezing during the 3 minutes test (5 out of 86 mice). In the OL and NOR test, we excluded animals showing very low explorative behavior: less than 10 seconds of direct objects exploration during the 15 minutes test (2 out of 113 mice for OL test and 4 out of 131 mice for NOR test).

Immunohistochemistry. Animals were deeply anesthetized and transcardially perfused with 4% paraformaldehyde in 100 mM phosphate buffer (PB), pH 7.4. Brains were collected, post-fixed for 24 h in the same fixative solution, cryo-preserved in 30% sucrose in PB and stored at −80 °C until use. Immunohistochemistry was performed on 30-μm coronal sections, with the following primary antibodies: rat anti-BrdU (clone BU1/75[ICR1], Abcam, catalog n°: ab6326; 1:200); rabbit anti-DCX (Abcam, catalog n°: ab18723; 1:1000); mouse anti-NeuN (clone A60, Millipore, catalog n°: MAB377; 1:250); rabbit anti-GFAP (Abcam, catalog n°: ab16997; 1:100); rabbit anti-vGAT (SYSY, catalog n°: 131-013; 1:700); guinea pig anti-vGLUT1 (SYSY, catalog n°: 135–304; 1:2500). Fluorophore conjugated (Alexa Fluor 488, Alexa Fluor 568, Alexa Fluor 647), goat secondary antibodies (1:1000; Invitrogen) were used for detection. The sections were counterstained with the nuclear dye Hoechst-33342 (Sigma-Aldrich). For BrdU immunohistochemistry, sections were pretreated with 2 N HCl as previously described[6].

For the assessment of dentate adult neurogenesis, stereological cell counting was performed in serial coronal sections (180 μm apart) covering the complete rostro-caudal extension of the dentate gyrus as previously described[6]. Fluorescence images were captured with a Nikon A1 confocal scanning microscope equipped with a 40X air objective and a motorized stage. For each section, confocal z-stack images (1 μm z-step size) covering the complete dentate gyrus were acquired and DG reconstructed with NIS Element AR software (Nikon). Immunolabeled cells in the granular cell layer (GCL) and the subgranular zone (SGZ, defined as a 10 μm region

below the GCL) were counted on the reconstructed images by an operator blind to the experimental groups according to the optical dissector principle[153].

For quantitative analyses of vGAT- and vGLUT1-positive puncta density, measurements were performed on images acquired with a SP5 confocal scanning microscope (Leica Microsystems), equipped with a 63X oil-immersion objective. Puncta density was evaluated on serial coronal sections (180 μm apart) covering the complete rostro-caudal extension of the hippocampus. Puncta immunostained for vGAT and vGLUT1 were automatically quantified in random fields of the CA1 stratum Radiatum on single-plain optical section images using the particle analysis plugin available in ImageJ software (http://imagej.nih.gov/ij/).

Electron Microscopy. Coronal brain slices (30 μm thickness) were post-fixed by immersion in 2% glutaraldehyde in 0,1 M sodium Cacodylate buffer (NaCacodylate, pH 7.4). Following aldehyde fixation, slices were rinsed in 0,1 M NaCacodylate buffer and further treated for 1 hours with 1% OsO4 in 1.5% $K_4Fe(CN)_6$ in 0.1 M NaCacodylate at room temperature, *en bloc* stained with 1% uranyl acetate for 45 minutes, dehydrated through a series of graded ethanol solutions, washed in propylene oxide and flat embedded in epoxy resin (Epon 812, TAAB) between two Aclar sheets. After 48 hours of polymerization at 60 °C, a small region corresponding to the hippocampal CA1 was excised from the blocks of resin and cut with an EM UC6 ultramicrotome (Leica Microsystem). Semi-thin section (0,5 μm thickness) was taken from each brain slice, stained with 1% of toluidine blue and analyzed at low magnification to identify the central region of CA1 stratum Radiatum. Ultrathin sections (70 nm thickness) were collected on 200 mesh copper grids and observed with a JEM-1011 microscope (Jeol) operating at 100 kV and equipped with an ORIUS SC1000 CCD camera (Gatan).

Symmetric (GABAergic) and asymmetric (glutamatergic) synapses were morphologically identified based on the shape of the presynaptic bouton and presence of thick and electron-dense post-synaptic density typical of glutamatergic terminals[154,155]. Synaptic bouton areas, length of the active zone (AZ), total and docked SV densities were calculated using ImageJ software. Total SV density was calculated on the total area of each presynaptic bouton. AZ was morphologically identified as the opposition region between pre- and post- synaptic structures with docked SV. Docked SV density was calculated on the length of the active zone of each presynaptic bouton. Only synapses with at least one docked synaptic vesicles were analyzed.

Biochemistry. Samples were lysed in ice-cold RIPA buffer (1% NP40, 0.5% Deoxycholic acid, 0.1% SDS, 150 mM NaCl, 1 mM EDTA, 50 mM Tris, pH 7.4) containing 1 mM PMSF, 10 mM NaF, 2 mM sodium orthovanadate and 1% (v/v) protease and phosphatase inhibitor cocktails (Sigma). Samples were clarified through centrifugation at *20,000* × *g* at 4 °C, and the protein concentration was determined using the BCA kit (Pierce). For immunoblot analysis, equal amounts of proteins were run on 4–12% Bis-Tris NuPAGE (Life Technologies) or Criterion-XT (Bio-Rad) gels and transferred overnight at 4 °C onto nitrocellulose membranes (GE Healthcare). Membranes were probed with rabbit anti-BDNF (Santa Cruz Biotechnology, catalog n°: sc-546; 1:500)[66], rabbit anti-phospho-$TrkB^{Tyr817}$ (Abcam, catalog n°: ab81288; 1:20000), rabbit anti-TrkB (Millipore, catalog n°: 07-225; 1:2000), and rabbit anti-Actin (Sigma, catalog n°: A2066; 1:10000), followed by HRP-conjugated goat secondary antibodies (Thermo Scientific) or fluorophore-conjugated (Cy3 or Cy5) goat secondary antibodies (GE Healthcare). Chemiluminescence signals were revealed with the SuperSignal West Pico substrate (Pierce) and digitally acquired on a LAS 4000 Mini imaging system (GE Healthcare). Fluorescent signals were acquired with Typhoon fluorescent scanner (GE Healthcare). Band intensities were quantified using ImageQuant software (GE Healthcare). For the determination of phospho-TrkB levels in brain lysates, membranes were first probed with the phospho-specific antibody, stripped and re-probed with a second antibody for total TrkB. The specificity of anti-BDNF antibody was verified by immunoblot analysis of recombinant BDNF (PeproTech) (Supplementary Fig. 4).

BDNF quantification by "sandwich" enzyme-linked immunosorbent assay (ELISA) was performed with BDNF E_{max} ImmunoAssay System (Promega) on 50 μg of hippocampal protein extracts (as above) according to the manufacturer's instructions. Absorbance at 450 nm was measured with a Victor3 plate reader (PerkinElmer).

Real Time Quantitative PCR (RT-qPCR). RT-qPCR was performed as previously described[15,156]. RNA was extracted with QIAzol reagent and purified on RNeasy spin columns (Qiagen), which includes an in-column RNAse-free DNAse digestion for the removal of contaminating genomic DNA. RNA samples were quantified at 260 nm with a ND1000 Nanodrop spectrophotometer (Thermo Scientific). RNA purity was also determined by absorbance at 280 and 230 nm. Reverse transcription was performed according to the manufacturer's recommendations on 1 μg of RNA with QuantiTect Reverse Transcription Kit (Qiagen). SYBR green RT-qPCR was performed in triplicate with 10 ng of template cDNA using QuantiTect master mix (Qiagen) on a 7900-HT Fast Real-time System (Applied Biosystem), using the following universal conditions: 5 min at 95 °C, 40 cycles of denaturation at 95 °C for 15 sec, and annealing/extension at 60 °C for 30 sec. Product specificity and occurrence of primer dimers were verified by melting curve analysis. Primers were designed with Beacon Designer software (Premier Biosoft) in order to avoid template secondary structure and significant cross homologies regions with other gene by BLAST search. For each target gene, primers were designed to target specific transcript variants annotated in RefSeq database (http://www.ncbi.nlm.nih.gov/refseq). In each experiment no-template controls (NTC) and RT-minus controls were run in parallel to the experimental samples. PCR reaction efficiency for each primer pair was calculated by the standard curve method with serial dilution of cDNA. PCR efficiency calculated for each primer set was used for subsequent analysis. All experimental samples were detected within the linear range of the assay. Gene expression data were normalized by the multiple internal control gene method[157]. To determine an accurate normalization factor for data analysis the expression stability of different control genes was evaluated with GeNorm algorithm[157] available in qBasePlus software (Biogazelle). The tested control genes were: GAPDH (glyceraldehyde-3-phosphate dehydrogenase), PPIA (peptidylprolyl isomerase A) and ACTB (β-actin).

Based on the relative expression stability of the control genes calculated by GeNorm analysis, expression data for the different samples were normalized with GAPDH and PPIA. However we noted that expression stability of the control genes was generally similar, therefore comparable expression results were obtained also by normalization with the other control genes. SYBR green primer sequences are reported in Supplementary Table 1. Calibration curves parameters, PCR reaction efficiency and amplicon information are listed in Supplementary Table 2.

Human Brain Samples. Hippocampal samples from adult human Down syndrome patients and age/sex-matched non-trisomic controls were obtained from the Brain and Tissue Bank for Developmental Disorders at the University of Maryland, Baltimore (MD). Samples information are described in Supplementary Table 3 and were previously reported[15]. Samples were cryo-pulverized in dry ice (−78 °C) with a stainless steel mortar. Aliquots of pulverized tissue were used for protein and RNA extraction.

Electrophysiology. *Field recordings.* For CA3-CA1 LTP mice were anesthetized with isoflurane and transcardially perfused with an ice-cold ACSF solution with the following composition (in mM): 120 NaCl, 3.5 KCl, 1.25 NaH_2PO_4, 1.3 $MgSO_4$, 2.5 $CaCl_2$, 26 $NaHCO_3$ and 10 glucose (pH 7.4), oxygenated with 95% O_2 and 5% CO_2[15,20]. The animal was sacrificed, and the brain was removed and immersed in ice-cold ACSF. Sagittal slices (400 μm) were prepared with a VT1000S vibratome (Leica Microsystems) and incubated at 35 °C for 20 minutes in oxygenated ACSF. After 2 h recovery at room temperature, slices were transferred to a recording chamber and perfused with ACSF (35 °C, 1.7 mL/min). Electrical stimulation (100 μs duration) of Shaffer collateral was achieved by a bipolar tungsten stimulating electrode (WPI, USA) placed in the stratum radiatum. Field excitatory post-synaptic potentials (fEPSPs) in CA1 stratum radiatum were recorded by a micropipette (1–3 MΩ) filled with ACSF. Baseline responses were obtained every 30 s with a stimulation intensity that yielded a half-maximal slope (mV/ms) response. After achievement of a 10 min stable baseline, a theta-burst stimulation (TBS) was delivered. The protocol of TBS stimulation consisted of 5 bursts at 5 Hz, each burst consisted of 4 pulses at 100 Hz[15,20]. Data, filtered at 0.1 Hz and 600 Hz and sampled at 25 kHz were acquired with a patch-clamp amplifier (Multiclamp 700B, Molecular Devices), and analyzed using pClamp 10.2 software (Molecular Devices).

For DG LTP mice were anesthetized with isoflurane and transcardially perfused with an ice-cold ACSF solution containing (in mM): 119 NaCl, 2.5 KCl, 1.3 $MgSO_4$, 1 NaH_2PO_4, 26 $NaHCO_3$, 2.5 $CaCl_2$, and 10 glucose (pH 7.4), oxygenated with 95% O_2 and 5% CO_2[6]. The animal was sacrificed, and the brain was removed and immersed in ice-cold ACSF. Transverse hippocampal slices (400 μm) were prepared using a Microm HM 650 V vibratome equipped with Microm CU 65 cooling unit (Thermo Scientific) and incubated at 32 °C for 30 minutes in oxygenated ACSF. Slice were then transferred into a holding chamber containing oxygenated ACSF and incubated for at least 90 minutes at room temperature before recording. The slices were transferred into a recording chamber and continuously perfused with oxygenated ACSF (2 ml/min) at 31 °C ± 1 °C. Afferent fibers on the media perforant path (MPP) were stimulated using a bipolar tungsten stimulating electrode (WPI, USA), and fEPSPs were recorded using glass capillary electrodes (4–5 MΩ) filled with ACSF positioned in the medial molecular layer of the upper blade of the DG. Baseline recordings were conducted with a frequency of 1 test stimulus every 30 seconds. Only slices showing fEPSPs of 1 mV in amplitude or higher were selected for experiments. LTP was induced through a tetanic stimulation that consisted of four 100-Hz trains of 0.5 seconds each repeated every 30 seconds. After induction, the responses were recorded every 30 seconds for at least 60 minutes. The data were 0.1–1000 Hz band-pass filtered and amplified using a DAM 80 amplifier (WPI), digitized at a sampling rate of 25 kHz using a Digidata 1440 A (Molecular Devices) running with Clampex software (Molecular Devices). The Clampfit software (Molecular Devices) was used for data analysis.

Patch-clamp recordings. Whole-cell patch-clamp recordings from CA1 pyramidal neurons were performed using Multiclamp 700B/Digidata1440A system (Molecular Devices, Sunnyvale CA, USA) and an upright Olympus BX51WI microscope (Olympus) equipped with Nomarski optics. After anesthetization with isoflurane, transverse hippocampal slices (400 μm) were cut using a Microm HM 650 V microtome equipped with Microm CU 65 cooling unit (Thermo Fisher Scientific). Slices were cut at 2 °C in a solution containing (in mM): 87 NaCl, 25 $NaHCO_3$, 2.5 KCl, 0.5 $CaCl_2$, 7 $MgCl_2$, 25 glucose, and 75 sucrose saturated with 95% O_2 and 5% CO_2. After cutting the slices were left to recover for 1 hour at 35 °C and for another 2 hours at room temperature in recording solution. Experiments were performed at 22–24 °C. The extracellular solution used for recordings contained (in mM): 125 NaCl, 25 $NaHCO_3$, 25 glucose, 2.5 KCl, 1.25 NaH_2PO_4, 2 $CaCl_2$, and 1 $MgCl_2$ (bubbled with 95% O_2-5% CO_2). All experiments were performed at a holding potential Vh = −70 mV in the presence of 0.3 μM TTX (Tocris Bioscience). Miniature excitatory postsynaptic currents (mEPSP) were recorded with an internal solution containing (in mM): 126 K gluconate, 4 NaCl, 1 $MgSO_4$, 0.02 $CaCl_2$, 0.1 BAPTA, 15 Glucose, 5 HEPES, 3 ATP, 0.1 GTP (pH 7.3) in the presence of 30 μM bicuculline and 5 μM CGP55845 (Tocris Bioscience) to block $GABA_A$ and $GABA_B$ receptors, respectively. Miniature inhibitory postsynaptic currents (mIPSP) were recorded with a high-chloride intracellular solution containing (in mM): 126 KCl, 4 NaCl, 1 $MgSO_4$, 0.02 $CaCl_2$, 0.1 BAPTA, 15 Glucose, 5 HEPES, 3 ATP and 0.1 GTP (pH 7.3) in the presence of 50 μM D-AP5 and 10 μM CNQX (Tocris Bioscience) to block NMDA and non-NMDA receptors, respectively. Somatic access resistance was monitored continuously, and cells with access resistance larger than 15 MΩ and/or a holding current larger than −200 pA were excluded. All patch-clamp data were acquired with Clampex 10.2 and analyzed offline with Clampfit 10.2 (pClamp, Molecular Devices) and MiniAnalysis (Synaptosoft).

Statistical analysis. The results are presented as the means ± SEM. The statistical analysis was performed using SigmaPlot (Systat) and GraphPad (Prism) software. Where appropriate, the statistical significance was assessed using the following parametric test: two-tailed unpaired t-test, two-way ANOVA or two-way repeated

measure ANOVA followed by all pairwise Turkey's *post hoc* test. In case normal distribution or equal variance assumptions were not valid, statistical significance was evaluated using Mann-Whitney test (non-parametric) or by two-way ANOVA on ranked transformed data. P values < 0.05 were considered significant.

Ethical approval declaration. A veterinarian was employed to monitor health and comfort of the animals. Mice were housed in a temperature-controlled room with a 12:12 hour dark/light cycle with *ad libitum* access to water and food. All animal experiments were performed in accordance with the guidelines established by the European Community Council Directive 2010/63/EU of September 22nd, 2010 and were approved by the Italian Ministry of Health (authorization n°: 216/2012-B and 658/2016-PR).

References

1. Dierssen, M. Down syndrome: the brain in trisomic mode. *Nature reviews. Neuroscience* **13**, 844–858 (2012).
2. Pennington, B. F., Moon, J., Edgin, J., Stedron, J. & Nadel, L. The neuropsychology of Down syndrome: evidence for hippocampal dysfunction. *Child Dev* **74**, 75–93 (2003).
3. Vicari, S., Pontillo, M. & Armando, M. Neurodevelopmental and psychiatric issues in Down's syndrome: assessment and intervention. *Psychiatr Genet* **23**, 95–107 (2013).
4. Edgin, J. O., Mason, G. M., Spanò, G., Fernández, A. & L. N. Human and mouse model cognitive phenotypes in Down syndrome: implications for assessment. *Prog Brain Res* **197**, 123–151 (2012).
5. Reeves, R. H. *et al*. A mouse model for Down syndrome exhibits learning and behaviour deficits. *Nat Genet* **11**, 177–184 (1995).
6. Contestabile, A. *et al*. Lithium rescues synaptic plasticity and memory in Down syndrome mice. *J Clin Invest* **123**, 348–361 (2013).
7. Costa, C. S. A., Scott-McKean, J. J. & Stasko, M. R. Acute Injections of the NMDA Receptor Antagonist Memantine Rescue Performance Deficits of the Ts65Dn Mouse Model of Down Syndrome on a Fear Conditioning Test. *Neuropsychopharmacology* **33**, 1624–1632 (2007).
8. Duchon, A. *et al*. Identification of the translocation breakpoints in the Ts65Dn and Ts1Cje mouse lines: relevance for modeling down syndrome. *Mamm Genome* **22**, 674–684, https://doi.org/10.1007/s00335-011-9356-0 (2011).
9. Gardiner, K. J. Pharmacological approaches to improving cognitive function in Down syndrome: current status and considerations. *Drug Des Devel Ther* **9**, 103–125 (2014).
10. Fernandez, F. *et al*. Pharmacotherapy for cognitive impairment in a mouse model of Down syndrome. *Nature Neuroscience* **10**, 411–413 (2007).
11. Kleschevnikov, A. M. *et al*. Hippocampal long-term potentiation suppressed by increased inhibition in the Ts65Dn mouse, a genetic model of Down syndrome. *J Neurosci* **24**, 8153–8160 (2004).
12. Hanson, J. E., Blank, M., Valenzuela, R. A., Garner, C. C. & Madison, D. V. The functional nature of synaptic circuitry is altered in area CA3 of the hippocampus in a mouse model of Down's syndrome. *J. Physiology* **579** (2007).
13. Best, T. K., Cramer, N. P., Chakrabarti, L., Haydar, T. F. & Galdzicki, Z. Dysfunctional hippocampal inhibition in the Ts65Dn mouse model of Down syndrome. *Experimental Neurology* (2012).
14. Kleschevnikov, A. M. *et al*. Increased efficiency of the GABAA and GABAB receptor-mediated neurotransmission in the Ts65Dn mouse model of Down syndrome. *Neurobiol Dis* **45**, 683–691 (2012).
15. Deidda, G. *et al*. Reversing excitatory GABAAR signaling restores synaptic plasticity and memory in a mouse model of Down syndrome. *Nature Medicine* **21**, 318–326 (2015).
16. Contestabile, A., Magara, S. & Cancedda, L. The GABAergic Hypothesis for Cognitive Disabilities in Down Syndrome. *Front Cell Neurosci* **11**, 54 (2017).
17. Stagni, F. *et al*. Pharmacotherapy with fluoxetine restores functional connectivity from the dentate gyrus to field CA3 in the Ts65Dn mouse model of down syndrome. *PLoS One* **8**, e61689 (2013).
18. Braudeau, J. *et al*. Specific targeting of the GABA-A receptor alpha5 subtype by a selective inverse agonist restores cognitive deficits in Down syndrome mice. *Journal of psychopharmacology* **25**, 1030–1042, https://doi.org/10.1177/0269881111405366 (2011).
19. Martinez-Cue, C. *et al*. Reducing GABAA alpha5 receptor-mediated inhibition rescues functional and neuromorphological deficits in a mouse model of down syndrome. *J Neurosci* **33**, 3953–3966, https://doi.org/10.1523/JNEUROSCI.1203-12.2013 (2013).
20. Costa, A. C. & Grybko, M. J. Deficits in hippocampal CA1 LTP induced by TBS but not HFS in the Ts65Dn mouse: a model of Down syndrome. *Neurosci Lett* **382**, 317–322 (2005).
21. Clark, S., Schwalbe, J., Stasko, M. R., Yarowsky, P. J. & Costa, A. C. Fluoxetine rescues deficient neurogenesis in hippocampus of the Ts65Dn mouse model for Down syndrome. *Exp Neurol* **200**, 256–261 (2006).
22. Mattson, M. P. Evolutionary aspects of human exercise–born to run purposefully. *Ageing research reviews* **11**, 347–352 (2012).
23. Cotman, C. W. & Berchtold, N. C. Exercise: a behavioral intervention to enhance brain health and plasticity. *Trends Neurosci* **25**, 295–301 (2002).
24. van Praag, H. Exercise and the brain: something to chew on. *Trends Neurosci* **32**, 283–290 (2009).
25. Hillman, C. H., Erickson, K. I. & Kramer, A. F. Be smart, exercise your heart: exercise effects on brain and cognition. *Nature reviews. Neuroscience* **9**, 58–65 (2008).
26. Intlekofer, K. A. & Cotman, C. W. Exercise counteracts declining hippocampal function in aging and Alzheimer's disease. *Neurobiol Dis* (2012).
27. Berchtold, N. C., Castello, N. & Cotman, C. W. Exercise and time-dependent benefits to learning and memory. *Neuroscience* **167**, 588–597 (2010).
28. Voss, M. W., Nagamatsu, L. S., Liu-Ambrose, T. & Kramer, A. F. Exercise, brain, and cognition across the life span. *Journal of applied physiology* **111**, 1505–1513 (2011).
29. Pereira, A. C. *et al*. An *in vivo* correlate of exercise-induced neurogenesis in the adult dentate gyrus. *Proc Natl Acad Sci USA* **104**, 5638–5643 (2007).
30. Erickson, K. I. *et al*. Exercise training increases size of hippocampus and improves memory. *PNAS* **108**, 3017–3322 (2011).
31. Erickson, K. I., Miller, D. L. & Roecklein, K. A. The aging hippocampus: interactions between exercise, depression, and BDNF. *The Neuroscientist: a review journal bringing neurobiology, neurology and psychiatry* **18**, 82–97, https://doi.org/10.1177/1073858410397054 (2012).
32. Zoladz, J. A. & Pilc, A. The effect of physical activity on the brain derived neurotrophic factor: from animal to human studies. *Journal of physiology and pharmacology: an official journal of the Polish Physiological Society* **61**, 533–541 (2010).
33. Voss, M. W. *et al*. The influence of aerobic fitness on cerebral white matter integrity and cognitive function in older adults: Results of a one-year exercise intervention. *Human brain mapping*. https://doi.org/10.1002/hbm.22119 (2012).
34. Kramer, A. F. *et al*. Enhancing brain and cognitive function of older adults through fitness training. *J Mol Neurosci* **20**, 213–221 (2003).
35. Colcombe, S. J. *et al*. Aerobic fitness reduces brain tissue loss in aging humans. *The journals of gerontology. Series A, Biological sciences and medical sciences* **58**, 176–180 (2003).
36. Smith, P. J. *et al*. Aerobic exercise and neurocognitive performance: a meta-analytic review of randomized controlled trials. *Psychosomatic medicine* **72**, 239–252 (2010).

37. Colcombe, S. & Kramer, A. F. Fitness effects on the cognitive function of older adults: a meta-analytic study. *Psychological science* **14**, 125–130 (2003).
38. van Praag, H. Neurogenesis and exercise: past and future directions. *Neuromolecular Med.* **10**, 128–140 (2008).
39. Herting, M. M. & Nagel, B. J. Aerobic fitness relates to learning on a virtual Morris Water Task and hippocampal volume in adolescents. *Behav Brain Res* **233**, 517–525 (2012).
40. Neeper, S. A., Gomez-Pinilla, F., Choi, J. & Cotman, C. Exercise and brain neurotrophins. *Nature* **373**, 109 (1995).
41. Berchtold, N. C., Chinn, G., Chou, M., Kesslak, J. P. & Cotman, C. W. Exercise primes a molecular memory for brain-derived neurotrophic factor protein induction in the rat hippocampus. *Neuroscience* **133**, 853–861 (2005).
42. van Praag, H., Shubert, T., Zhao, C. & Gage, F. H. Exercise Enhances Learning and Hippocampal Neurogenesisin Aged Mice. *Journal of Nuroscience* **25**, 8680–8685 (2005).
43. Olson, A. K., Eadie, B. D., Ernst, C. & Christie, B. R. Environmental enrichment and voluntary exercise massively increase neurogenesis in the adult hippocampus via dissociable pathways. *Hippocampus* **16**, 250–260 (2006).
44. Farmer, J. *et al*. Effects of voluntary exercise on synaptic plasticity and gene expression in the dentate gyrus of adult male Sprague-Dawley rats *in vivo*. *Neuroscience* **124**, 71–79 (2004).
45. Yau, S. Y. *et al*. Hippocampal neurogenesis and dendritic plasticity support running-improved spatial learning and depression-like behaviour in stressed rats. *Plos One* **6**, e24263 (2011).
46. van Praag, H., Kempermann, G. & Gage, F. H. Running increases cell proliferation and neurogenesis in the adult mouse dentate gyrus. *Nat Neurosci*, 266-270 (1999).
47. Vaynman, S., Ying, Z. & Gomez-Pinilla, F. Hippocampal BDNF mediates the efficacy of exercise on synaptic plasticity and cognition. *European Journal of Neuroscience* **20**, 2580–2590 (2004).
48. van Praag, H., Christie, B. R., Sejnowski, T. J. & Gage, F. H. Running enhances neurogenesis, learning, and long-term potentiation in mice. *Proc Natl Acad Sci USA* **96**, 13427–13431 (1999).
49. Li, Y. *et al*. TrkB regulates hippocampal neurogenesis and governs sensitivity to antidepressive treatment. *Neuron* **59**, 399–412 (2008).
50. Gomez-Pinilla, F., Vaynman, S. & Ying, Z. Brain-derived neurotrophic factor functions as a metabotrophin to mediate the effects of exercise on cognition. *Eur J Neurosci* **28**, 2278–2287 (2008).
51. Bekinschtein, P., Oomen, C. A., Saksida, L. M. & Bussey, T. J. Effects of environmental enrichment and voluntary exercise on neurogenesis, learning and memory, and pattern separation: BDNF as a critical variable? *Semin Cell Dev Biol* **22**, 536–542 (2011).
52. Griffin, E. W., Bechara, R. G., Birch, A. M. & Kelly, A. M. Exercise enhances hippocampal-dependent learning in the rat: evidence for a BDNF-related mechanism. *Hippocampus* **19**, 973–980 (2009).
53. Figurov, A., Pozzo-Miller, L. D., Olafsson, P., Wang, T. & Lu, B. Regulation of synaptic responses to high-frequency stimulation and LTP by neurotrophins in the hippocampus. *Nature* **381**, 706–709 (1996).
54. Korte, M. *et al*. Hippocampal long-term potentiation is impaired in mice lacking brain-derived neurotrophic factor. *Proc Natl Acad Sci USA* **92**, 8856–8860 (1995).
55. Patterson, S. L. *et al*. Recombinant BDNF rescues deficits in basal synaptic transmission and hippocampal LTP in BDNF knockout mice. *Neuron* **16**, 1137–1145 (1996).
56. Linnarsson, S., Bjorklund, A. & Ernfors, P. Learning deficit in BDNF mutant mice. *Eur J Neurosci* **9**, 2581–2587 (1997).
57. Mizuno, M., Yamada, K., Olariu, A., Nawa, H. & Nabeshima, T. Involvement of brain-derived neurotrophic factor in spatial memory formation and maintenance in a radial arm maze test in rats. *J Neurosci* **20**, 7116–7121 (2000).
58. Minichiello, L. *et al*. Essential role for TrkB receptors in hippocampus-mediated learning. *Neuron* **24**, 401–414 (1999).
59. Heldt, S. A., Stanek, L., Chhatwal, J. P. & Ressler, K. J. Hippocampus-specific deletion of BDNF in adult mice impairs spatial memory and extinction of aversive memories. *Mol Psychiatry* **12**, 656–670 (2007).
60. Alonso, M. *et al*. BDNF-triggered events in the rat hippocampus are required for both short- and long-term memory formation. *Hippocampus* **12**, 551–560 (2002).
61. Lee, J. L., Everitt, B. J. & Thomas, K. L. Independent cellular processes for hippocampal memory consolidation and reconsolidation. *Science* **304**, 839–843 (2004).
62. Bekinschtein, P. *et al*. BDNF is essential to promote persistence of long-term memory storage. *Proc Natl Acad Sci USA* **105**, 2711–2716 (2008).
63. Bergami, M. *et al*. Deletion of TrkB in adult progenitors alters newborn neuron integration into hippocampal circuits and increases anxiety-like behavior. *Proc Natl Acad Sci USA* **105**, 15570–15575 (2008).
64. Waterhouse, E. G. *et al*. BDNF promotes differentiation and maturation of adult-born neurons through GABAergic transmission. *J Neurosci* **32**, 14318–14330 (2012).
65. Begenisic, T., Sansevero, G., Baroncelli, L., Cioni, G. & A. S. Early environmental therapy rescues brain development in a mouse model of Down syndrome. *Neurobiol Dis* **82**, 409–419 (2015).
66. Kleschevnikov, A. M. *et al*. Deficits in cognition and synaptic plasticity in a mouse model of Down syndrome ameliorated by GABAB receptor antagonists. *J Neurosci* **32**, 9217–9227 (2012).
67. Lockrow, J., Bogera, H., Bimonte-Nelson, H. & Granholm, A. C. Effects of long-term memantine on memory and neuropathology in Ts65Dn mice, a model for Down syndrome. *Behavioural Brain Research* **221**, 610–622 (2011).
68. Bechara, R. G. & Kelly, A. M. Exercise improves object recognition memory and induces BDNF expression and cell proliferation in cognitively enriched rats. *Behav Brain Res* **245**, 96–100 (2013).
69. Hopkins, M. E., Nitecki, R. & Bucci, D. J. Physical exercise during adolescence versus adulthood: differential effects on object recognition memory and brain-derived neurotrophic factor levels. *Neuroscience* **194**, 84–94 (2011).
70. Deng, W., Aimone, J. B. & Gage, F. H. New neurons and new memories: how does adult hippocampal neurogenesis affect learning and memory? *Nature reviews. Neuroscience* **11**, 339–350 (2010).
71. Kempermann, G., Kuhn, H. G. & Gage, F. H. More hippocampal neurons in adult mice living in an enriched environment. *Nature* **386**, 493–495 (1997).
72. Parent, J. M. *et al*. Dentate granule cell neurogenesis is increased by seizures and contributes to aberrant network reorganization in the adult rat hippocampus. *J Neurosci* **17**, 3727–3738 (1997).
73. Brown, J. P. *et al*. Transient expression of doublecortin during adult neurogenesis. *J Comp Neurol* **467**, 1–10 (2003).
74. Snyder, J. S., Kee, N. & Wojtowicz, J. M. Effects of Adult Neurogenesis on Synaptic Plasticity in the Rat Dentate Gyrus. *J Neurophysiol* **85**, 2423–2431 (2001).
75. Saxe, M. D. *et al*. Ablation of hippocampal neurogenesis impairs contextual fear conditioning and synaptic plasticity in the dentate gyrus. *PNAS* **103**, 17501–17506 (2006).
76. Sahay, A. *et al*. Increasing adult hippocampal neurogenesis is sufficient to improve pattern separation. *Nature* **472**, 466–470, https://doi.org/10.1038/nature09817 (2011).
77. Ge, S., Yang, C., Hsu, K., Ming, G. & Song, H. A Critical Period for Enhanced Synaptic Plasticity in Newly Generated Neurons of the Adult Brain. *Neuron* **54**, 559–566 (2007).
78. Chakrabarti, L. *et al*. Olig1 and Olig2 triplication causes developmental brain defects in Down syndrome. *Nat Neurosci* **13**, 927–934 (2010).
79. Kobilo, T. *et al*. Running is the neurogenic and neurotrophic stimulus in environmental enrichment. *Learn Mem* **18**, 605–609 (2011).

80. Aid, T., Kazantseva, A., Piirsoo, M., Palm, K. & Timmusk, T. Mouse and Rat BDNF Gene Structure and Expression Revisited. *Journal of Neuroscience Research* **85**, 525–535 (2007).
81. Liu, Q. *et al*. Rodent BDNF genes, novel promoters, novel splice variants, and regulation by cocaine. *BRAIN RESEARCH* **1067**, 1–12 (2006).
82. Oliff, H. S., Berchtold, N. C., Isackson, P. & Cotman, C. W. Exercise-induced regulation of brain-derived neurotrophic factor (BDNF) transcripts in the rat hippocampus. *Brain Res Mol Brain Res* **61**, 147–153 (1998).
83. Liu, X. *et al*. O-Methylated Metabolite of 7,8-Dihydroxyflavone Activates TrkB Receptor and Displays Antidepressant Activity. *Pharmacology* **91**, 185–200 (2013).
84. Jang, S. W. *et al*. A selective TrkB agonist with potent neurotrophic activities by 7,8-dihydroxyflavone. *Proc Natl Acad Sci USA* **107**, 2687–2692 (2010).
85. Liu, X. *et al*. A Synthetic 7,8-Dihydroxyflavone Derivative Promotes Neurogenesis and Exhibits Potent Antidepressant Effect. *J Med Chem* **53**, 8274–8286 (2010).
86. Andero, R. *et al*. Effect of 7,8-dihydroxyflavone, a small-molecule TrkB agonist, on emotional learning. *Am J Psychiatry* **168**, 163–172 (2011).
87. Jiang, M. *et al*. Small-molecule TrkB receptor agonists improve motor function and extend survival in a mouse model of Huntington's disease. *Hum Mol Genet* **22**, 2462–2470 (2013).
88. Zhang, Z. *et al*. 7,8-dihydroxyflavone prevents synaptic loss and memory deficits in a mouse model of Alzheimer's disease. *Neuropsychopharmacology* **39**, 638–650 (2014).
89. Devi, L. & Ohno, M. 7,8-dihydroxyflavone, a small-molecule TrkB agonist, reverses memory deficits and BACE1 elevation in a mouse model of Alzheimer's disease. *Neuropsychopharmacology* **37**, 434–444 (2012).
90. Tan, Y. *et al*. 7,8-Dihydroxyflavone Ameliorates Cognitive Impairment by Inhibiting Expression of Tau Pathology in ApoE-Knockout Mice. *Front Aging Neurosci* **8**, 287, https://doi.org/10.3389/fnagi.2016.00287 (2016).
91. Zhang, M. W., Zhang, S. F., Li, Z. H. & Han, F. 7,8-Dihydroxyflavone reverses the depressive symptoms in mouse chronic mild stress. *Neurosci Lett* **635**, 33–38, https://doi.org/10.1016/j.neulet.2016.10.035 (2016).
92. Gao, L. *et al*. TrkB activation by 7,8-dihydroxyflavone increases synapse AMPA subunits and ameliorates spatial memory deficits in a mouse model of Alzheimer's disease. *J Neurochem* **136**, 620–636 (2016).
93. Agrawal, R. *et al*. Flavonoid derivative 7,8-DHF attenuates TBI pathology via TrkB activation. *Biochim Biophys Acta* **1852**, 862–872, https://doi.org/10.1016/j.bbadis.2015.01.018 (2015).
94. Sconce, M. D., Churchill, M. J., Moore, C. & Meshul, C. K. Intervention with 7,8-dihydroxyflavone blocks further striatal terminal loss and restores motor deficits in a progressive mouse model of Parkinson's disease. *Neuroscience* **290**, 454–471, https://doi.org/10.1016/j.neuroscience.2014.12.080 (2015).
95. Hsiao, Y. H., Hung, H. C., Chen, S. H. & Gean, P. W. Social interaction rescues memory deficit in an animal model of Alzheimer's disease by increasing BDNF-dependent hippocampal neurogenesis. *J Neurosci* **34**, 16207–16219, https://doi.org/10.1523/JNEUROSCI.0747-14.2014 (2014).
96. Chapman, R. S. & Hesketh, L. J. Behavioral phenotype of individuals with Down syndrome. *Ment Retard Dev Disabil Res Rev* **6**, 84–95 (2000).
97. Epstein, C. J. 2001 William Allan Award Address. From Down syndrome to the "human" in "human genetics". *Am J Hum Genet* **70**, 300–313 (2002).
98. Roizen, N. J. & Patterson, D. Down's syndrome. *Lancet* **361**, 1281–1289 (2003).
99. Vicari, S. Memory development and intellectual disabilities. *Acta Paediatr Suppl* **93**, 60–63, discussion 63–64 (2004).
100. Vicari, S., Bellucci, S. & Carlesimo, G. A. Implicit and explicit memory: a functional dissociation in persons with Down syndrome. *Neuropsychologia* **38**, 240–251 (2000).
101. Vicari, S., Bellucci, S. & Carlesimo, G. A. Visual and spatial long-term memory: differential pattern of impairments in Williams and Down syndromes. *Dev Med Child Neurol* **47**, 305–311 (2005).
102. Sylvester, P. E. The hippocampus in Down's syndrome. *J Ment Defic Res* **27**(Pt 3), 227–236 (1983).
103. Aylward, E. H. *et al*. MRI volumes of the hippocampus and amygdala in adults with Down's syndrome with and without dementia. *Am J Psychiatry* **156**, 564–568 (1999).
104. Pinter, J. D., Eliez, S., Schmitt, J. E., Capone, G. T. & Reiss, A. L. Neuroanatomy of Down's syndrome: a high-resolution MRI study. *Am J Psychiatry* **158**, 1659–1665 (2001).
105. Krasuski, J. S., Alexander, G. E., Horwitz, B., rapoport, S. I. & Schapiro, M. B. Relation of Medial Temporal Lobe Volumes to Age and Memory Function in Nondemented Adults With Down's Syndrome: Implications for the Prodromal Phase of Alzheimer's Disease. *Am J Psychiatry* **159**, 74–81 (2002).
106. De la Torre, R. *et al*. Epigallocatechin-3-gallate, a DYRK1A inhibitor, rescues cognitive deficits in Down syndrome mouse models and in humans. *Molecular nutrition & food research* **58**, 278–288 (2014).
107. Guidi, S. *et al*. Early pharmacotherapy with fluoxetine rescues dendritic pathology in the Ts65Dn mouse model of down syndrome. *Brain Pathol* **23**, 129–143 (2013).
108. Lu, B., Nagappan, G., Guan, X., Nathan, P. J. & Wren, P. BDNF-based synaptic repair as a disease-modifying strategy for neurodegenerative diseases. *Nature reviews. Neuroscience* **14**, 401–416 (2013).
109. Llorens-Martin, M. V. *et al*. Effects of voluntary physical exercise on adult hippocampal neurogenesis and behavior of Ts65Dn mice, a model of Down syndrome. *Neuroscience* **171**, 1228–1240 (2010).
110. Kida, E., Rabe, A., Walus, M., Albertini, G. & Golabek, A. A. Long-term running alleviates some behavioral and molecular abnormalities in Down syndrome mouse model Ts65Dn. *Exp Neurol* **240**, 178–189 (2013).
111. Velazquez, R. *et al*. Maternal choline supplementation improves spatial learning and adult hippocampal neurogenesis in the Ts65Dn mouse model of Down syndrome. *Neurobiology of Disease* **58**, 92–101 (2013).
112. Corrales, A. *et al*. Chronic melatonin treatment rescues electrophysiological and neuromorphological deficits in a mouse model of Down syndrome. *J Pineal Res* **56**, 51–61 (2013).
113. Chakrabarti, L., Galdzicki, Z. & Haydar, T. F. Defects in embryonic neurogenesis and initial synapse formation in the forebrain of the Ts65Dn mouse model of Down syndrome. *J. Neuroscience* **27**, 11483–11495 (2007).
114. Kurt, A. M., Kafa, I. M., Dierssen, M. & Davies, C. D. Deficits of neuronal density in CA1 and synaptic density in the dentate gyrus, CA3 and CA1, in a mouse model of Down syndrome. *Brain Res* **1022**, 101–109 (2004).
115. Kurt, M. A., Davies, D. C., Kidd, M., Dierssen, M. & Florez, J. Synaptic deficit in the temporal cortex of partial trisomy 16 (Ts65Dn) mice. *Brain Res* **858**, 191–197 (2000).
116. Rueda, N. *et al*. Memantine normalizes several phenotypic features in the Ts65Dn mouse model of Down syndrome. *J Alzheimers Dis* **21**, 277–290 (2010).
117. García-Cerro, S. *et al*. Overexpression of Dyrk1A is implicated in several cognitive, electrophysiological and neuromorphological alterations found in a mouse model of Down syndrome. *PLoS One* **9**, e106572 (2014).
118. Branco, T., Marra, V. & Staras, K. Examining size-strength relationships at hippocampal synapses using an ultrastructural measurement of synaptic release probability. *J Struct Biol* **172**, 203–210 (2010).
119. Murthy, V. N., Schikorski, T., Stevens, C. F. & Zhu, Y. Inactivity Produces Increases in Neurotransmitter Release and Synapse Size. *Neuron* **32**, 673–682 (2001).

120. Belichenko, P. V. *et al.* Excitatory-inhibitory relationship in the fascia dentata in the Ts65Dn mouse model of Down syndrome. *J Comp Neurol* **512**, 453–466, https://doi.org/10.1002/cne.21895 (2009).
121. Belichenko, P. V. *et al.* Synaptic structural abnormalities in the Ts65Dn mouse model of Down Syndrome. *J Comp Neurol* **480**, 281–298 (2004).
122. Rossi, C. *et al.* Brain-derived neurotrophic factor (BDNF) is required for the enhancement of hippocampal neurogenesis following environmental enrichment. *Eur J Neurosci*, 1850–1856 (2006).
123. Sale, A., Berardi, N. & Maffei, L. Enrich the environment to empower the brain. *Trends Neurosci* **32**, 233–239 (2009).
124. Begenisic, T. *et al.* Environmental enrichment decreases GABAergic inhibition and improves cognitive abilities, synaptic plasticity, and visual functions in a mouse model of Down syndrome. *Front Cell Neurosci* **5**, 29, https://doi.org/10.3389/fncel.2011.00029 (2011).
125. Mustroph, M. L. *et al.* Aerobic exercise is the critical variable in an enriched environment that increases hippocampal neurogenesis and water maze learning in male C57BL/6 J mice. *Neuroscience* **219**, 62–71 (2012).
126. Catuara-Solarz, S. *et al.* Principal Component Analysis of the Effects of Environmental Enrichment and (-)-epigallocatechin-3-gallate on Age-Associated Learning Deficits in a Mouse Model of Down Syndrome. *Front Behav Neurosci* **9**, 330 (2015).
127. de la Torre, R. *et al.* Safety and efficacy of cognitive training plus epigallocatechin-3-gallate in young adults with Down's syndrome (TESDAD): a double-blind, randomised, placebo-controlled, phase 2 trial. *Lancet Neurol* **15**, 801–810, https://doi.org/10.1016/S1474-4422(16)30034-5 (2016).
128. Ringenbach, S. D. *et al.* The effects of assisted cycling therapy (ACT) and voluntary cycling on reaction time and measures of executive function in adolescents with Down syndrome. *J Intellect Disabil Res* **60**, 1073–1085 (2016).
129. Chen, C. C. & Ringenbach, S. D. Dose-response relationship between intensity of exercise and cognitive performance in individuals with Down syndrome: a preliminary study. *J Intellect Disabil Res* **60**, 606–614 (2016).
130. Holzapfel, S. D. *et al.* Improvements in manual dexterity relate to improvements in cognitive planning after assisted cycling therapy (ACT) in adolescents with down syndrome. *Res Dev Disabil* **45-46**, 261–270 (2015).
131. Bimonte-Nelson, H. A., Hunter, C. L., Nelson, M. E. & Granholm, A. C. Frontal cortex BDNF levels correlate with working memory in an animal model of Down syndrome. *Behav Brain Res* **139**, 47–57 (2003).
132. Alldred, M. J., Lee, S. H., Petkova, E. & Ginsberg, S. D. Expression profile analysis of vulnerable CA1 pyramidal neurons in young-Middle-Aged Ts65Dn mice. *J Comp Neurol* **523**, 61–74 (2015).
133. Alldred, M. J., Lee, S. H., Petkova, E. & Ginsberg, S. D. Expression profile analysis of hippocampal CA1 pyramidal neurons in aged Ts65Dn mice, a model of Down syndrome (DS) and Alzheimer's disease (AD). *Brain Struct Funct* **220**, 2983–2996 (2015).
134. Fukuda, Y. *et al.* Stimulated neuronal expression of brain-derived neurotrophic factor by Neurotropin. *Mol Cell Neurosci* **45**, 226–233, https://doi.org/10.1016/j.mcn.2010.06.013 (2010).
135. Stagni, F. *et al.* Long-term effects of neonatal treatment with fluoxetine on cognitive performance in Ts65Dn mice. *Neurobiology of Disease* **74**, 204–218 (2015).
136. Bianchi, P. *et al.* Early pharmacotherapy restores neurogenesis and cognitive performance in the Ts65Dn mouse model for Down syndrome. *Journal of Neuroscience* **30**, 8769–8779 (2010).
137. Kazim, S. F., Blanchard, J., Bianchi, R. & Iqbal, K. Early neurotrophic pharmacotherapy rescues developmental delay and Alzheimer's-like memory deficits in the Ts65Dn mouse model of Down syndrome. *Scientific reports* **7**, 45561 (2017).
138. Bakos, J. *et al.* Enriched environment influences hormonal status and hippocampal brain derived neurotrophic factor in a sex dependent manner. *Neuroscience* **164**, 788–797 (2009).
139. Berchtold, N. C., Oliff, H. S., Isackson, P. & Cotman, C. W. Hippocampal BDNF mRNA shows a diurnal regulation, primarily in the exon III transcript. *Brain Res Mol Brain Res* **71**, 11–22 (1999).
140. Kesslak, J. P., So, V., Choi, J., Cotman, C. W. & Gomez-Pinilla, F. Learning upregulates brain-derived neurotrophic factor messenger ribonucleic acid: a mechanism to facilitate encoding and circuit maintenance? *Behav Neurosci* **112**, 1012–1019 (1998).
141. Hall, J., Thomas, K. L. & Everitt, B. J. Rapid and selective induction of BDNF expression in the hippocampus during contextual learning. *Nat Neurosci* **3**, 533–535 (2000).
142. Falkenberg, T. *et al.* Increased expression of brain-derived neurotrophic factor mRNA in rat hippocampus is associated with improved spatial memory and enriched environment. *Neurosci Lett* **138**, 153–156 (1992).
143. Tlili, A. *et al.* BDNF and DYRK1A are variable and inversely correlated in lymphoblastoid cell lines from Down syndrome patients. *Molecular neurobiology* **46**, 297–303 (2012).
144. Minichiello, L. TrkB signalling pathways in LTP and learning. *Nature reviews. Neuroscience* **10**, 850–860, https://doi.org/10.1038/nrn2738 (2009).
145. Edelmann, E., Lebmann, V. & Brigadski, T. Pre- and postsynaptic twists in BDNF secretion and action in synaptic plasticity. *Neuropharmacology* **76**, 610–627 (2014).
146. Harward, S. C. *et al.* Autocrine BDNF-TrkB signalling within a single dendritic spine. *Nature* **538**, 99–103 (2016).
147. Leal, G., Comprido, D. & Duarte, C. B. BDNF-induced local protein synthesis and synaptic plasticity. *Neuropharmacology* **76**, 639–656 (2014).
148. Nosheny, R. L. *et al.* Increased cortical synaptic activation of TrkB and downstream signaling markers in a mouse model of Down Syndrome. *Neurobiol Dis* **77**, 173–190 (2015).
149. Johnson, R. A. *et al.* 7,8-dihydroxyflavone exhibits therapeutic efficacy in a mouse model of Rett syndrome. *Journal of applied physiology* **112**, 704–710 (2012).
150. He, J. *et al.* Neuroprotective Effects of 7,8-dihydroxyflavone on Midbrain Dopaminergic Neurons in MPP+ -treated Monkeys. *Scientific reports* **6**, 34339 (2016).
151. Zhang, J. C. *et al.* Antidepressant effects of TrkB ligands on depression-like behavior and dendritic changes in mice after inflammation. *Int J Neuropsychopharmacol* **18**, https://doi.org/10.1093/ijnp/pyu077 (2014).
152. Castello, N. A. *et al.* 7,8-Dihydroxyflavone, a small molecule TrkB agonist, improves spatial memory and increases thin spine density in a mouse model of Alzheimer disease-like neuronal loss. *PLoS One* **9**, e91453 (2014).
153. Kempermann, G., Gast, D., Kronenberg, G., Yamaguchi, M. & Gage, F. H. Early determination and long-term persistence of adult-generated new neurons in the hippocampus of mice. *Development* **130**, 391–399 (2003).
154. Ziff, E. B. Enlightening the postsynaptic density. *Neuron* **19**, 1163–1174 (1997).
155. Sheng, M. & Kim, E. The Postsynaptic Organization of Synapses. *Cold Spring Harb Perspect Biol* **3**, a005678 (2011).
156. Pozzi, D. *et al.* REST/NRSF-mediated intrinsic homeostasis protects neuronal networks from hyperexcitability. *EMBO J* **32**, 2994–3007, emboj2013231 [pii] 10.1038/emboj.2013.231 (2013).
157. Vandesompele, J. *et al.* Accurate normalization of real-time quantitative RT-PCR data by geometric averaging of multiple internal control genes. *Genome Biol* **3**, RESEARCH0034 (2002).

Acknowledgements

This work was supported by Jérôme Lejeune Foundation grant 254-CA2014A and Telethon Foundation grant GGP15043 to A.C. Human Down syndrome and control samples were obtained from the Brain and Tissue Bank for Developmental Disorders at the University of Maryland, Baltimore (MD). We thank the IIT animal facility staff for their valuable work.

Author Contributions

M.P. collected and analyzed the behavioral and immunohistochemistry data; D.G. L.M. and G.D. collected and analyzed the electrophysiology data; E.C. collected and analyzed the electron microscopy data; M.A. and M.P. collected and analyzed the biochemical data; P.B. and L.C. supervised the electrophysiology experiments; L.C. critically discussed the data and contributed in manuscript preparation; M.P. and A.C. prepared the figures. A.C. designed the experiments and wrote the manuscript. All authors read and revised the manuscript.

Additional Information

Supplementary information accompanies this paper at https://doi.org/10.1038/s41598-017-17201-8.

Competing Interests: The authors declare that they have no competing interests.

Publisher's note: Springer Nature remains neutral with regard to jurisdictional claims in published maps and institutional affiliations.

Supplementary information for:

Aerobic exercise and a BDNF-mimetic therapy rescue learning and memory in a mouse model of Down syndrome

Martina Parrini[1], Diego Ghezzi[1†], Gabriele Deidda[1§], Lucian Medrihan[1^], Enrico Castroflorio[2], Micol Alberti[1], Pietro Baldelli[2,3], Laura Cancedda[1] and Andrea Contestabile[1*].

[1] Department of Neuroscience and Brain Technologies, Istituto Italiano di Tecnologia, Genova, Italy.

[2] Center for Synaptic Neuroscience, Istituto Italiano di Tecnologia, Genova, Italy.

[3] Department of Experimental Medicine, University of Genova, Italy.

[†] Present address: Medtronic Chair in Neuroengineering, Center for Neuroprosthetics, Institute of Bioengineering, School of Engineering, École Polytechnique Fédérale de Lausanne, Switzerland

^ Present address: Laboratory of Molecular and Cellular Neuroscience, Rockefeller University, NY, USA.

[§] Present address: School of Biosciences, Cardiff University, UK.

*Corresponding author, andrea.contestabile@iit.it

Supplementary text and figures:

A

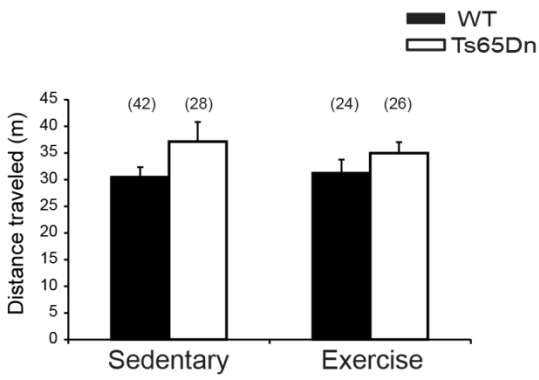

Supplementary Figure 1

Supplementary Figure 1. Physical exercise had no effect on general motor activity. **(A)** Distance traveled in the empty arena was not different across genotype and treatments. Two-way ANOVA on ranked transformed data: genotype [$F_{1,116}$ = 4.460, P = 0.037], treatment [$F_{1,116}$ = 0.038, P = 0.845], genotype x treatment [$F_{1,116}$ = 0.015, P = 0.901]. Tukey *post hoc* test following two-way ANOVA did not reach statistical significance for any experimental group. Number in parenthesis indicates the number of mice tested for each experimental group.

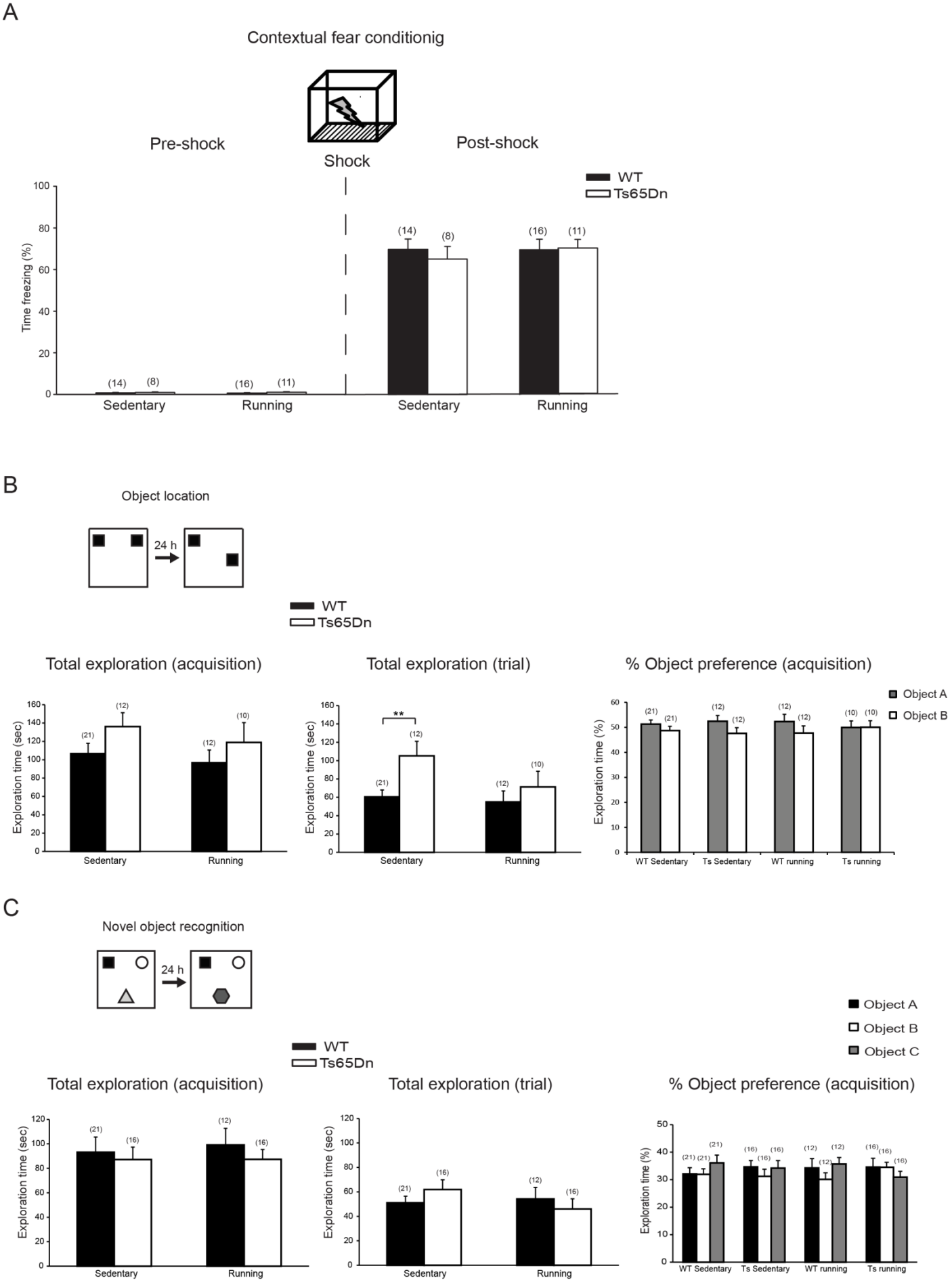

Supplementary Figure 2

Supplementary Figure 2. **(A)** Physical exercise had no effect on the freezing time before (left) or immediately after (right) the electric foot shock during the conditioning session in both Ts65Dn and WT mice. Pre-shock two-way ANOVA on ranked transformed data: genotype [$F_{1,45}$=1.964, P=0.168]; treatment [$F_{1,45}$=0.0661, P=0.798]; genotype x treatment [$F_{1,45}$=0.00002, P=0.996]. Post-shock two-way ANOVA: genotype [$F_{1,45}$=0.171, P=0.681]; treatment [$F_{1,45}$= 0.169, P=0.683]; genotype x treatment [$F_{1,45}$=0.194, P=0.661]. **(B)** *Left:* in the OL test the total exploration time during the acquisition phase was not significantly different across genotype and treatment. Two-way ANOVA: genotype [$F_{1,51}$=5.017, P=0.029]; treatment [$F_{1,51}$=0.641, P=0.427]; genotype x treatment [$F_{1,51}$=0.0223, P=0.882]. *Center*: the total exploration time during the trial phase was slightly increased in sedentary Ts65Dn mice compared to WT, however no significant difference was observed in Ts65Dn running mice compared to WT. Two-way ANOVA: genotype [$F_{1,51}$=9.164, P=0.004]; treatment [$F_{1,51}$=2.453, P=0.123]; genotype x treatment [$F_{1,51}$=0.914, P=0.349]. **P<0.01, Tukey post hoc test. *Right*: the percentage of time spent exploring the two objects during the acquisition phase was not statistically different across the experimental groups. Two-way ANOVA: genotype [$F_{1,102}$<0.0001, P=1.000]; treatment [$F_{1,102}$=1.331, P=0.268]; genotype x treatment [$F_{1,102}$=0.4014, P=0.753]. **(C)** *Left:* in the NOR test the total exploration time during the acquisition phases was not significantly different across genotype and treatment. Two-way ANOVA on ranked transformed data: genotype [$F_{1,61}$=0.585; P=0.447]; treatment [$F_{1,61}$=0.548; P=0.462]; genotype x treatment [$F_{1,61}$=0.0997; P=0.753]. *Center*: the total exploration time during the trial phase was not significantly different across genotype and treatment. Two-way ANOVA on ranked transformed data: genotype [$F_{1,61}$=0.0226; P=0.881]; treatment [$F_{1,61}$=1.892; P=0.174]; genotype x treatment [$F_{1,61}$=2.047; P=0.158]. *Right*: the percentage of time spent exploring the three objects during the acquisition phase was not statistically different across the experimental groups. Two-way ANOVA: genotype [$F_{1,187}$=0.231; P=0.645]; treatment [$F_{1,187}$=0.718; P=0.629]; genotype x treatment [$F_{1,187}$=0.895; P=0.521]. Number in parenthesis indicates the number of mice tested for each experimental group.

Asymmetric synapses (Glutamatergic)

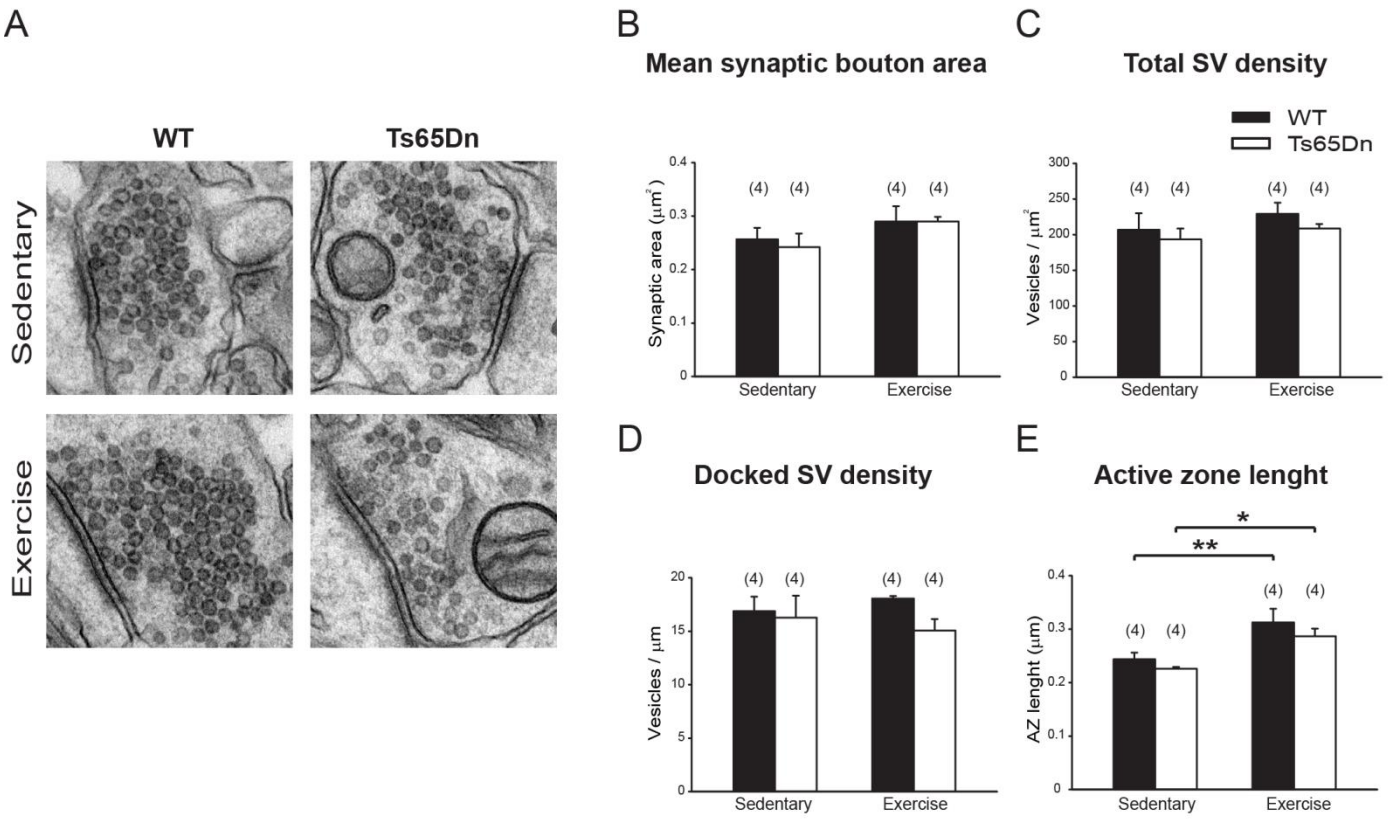

Symmetric synapses (GABAergic)

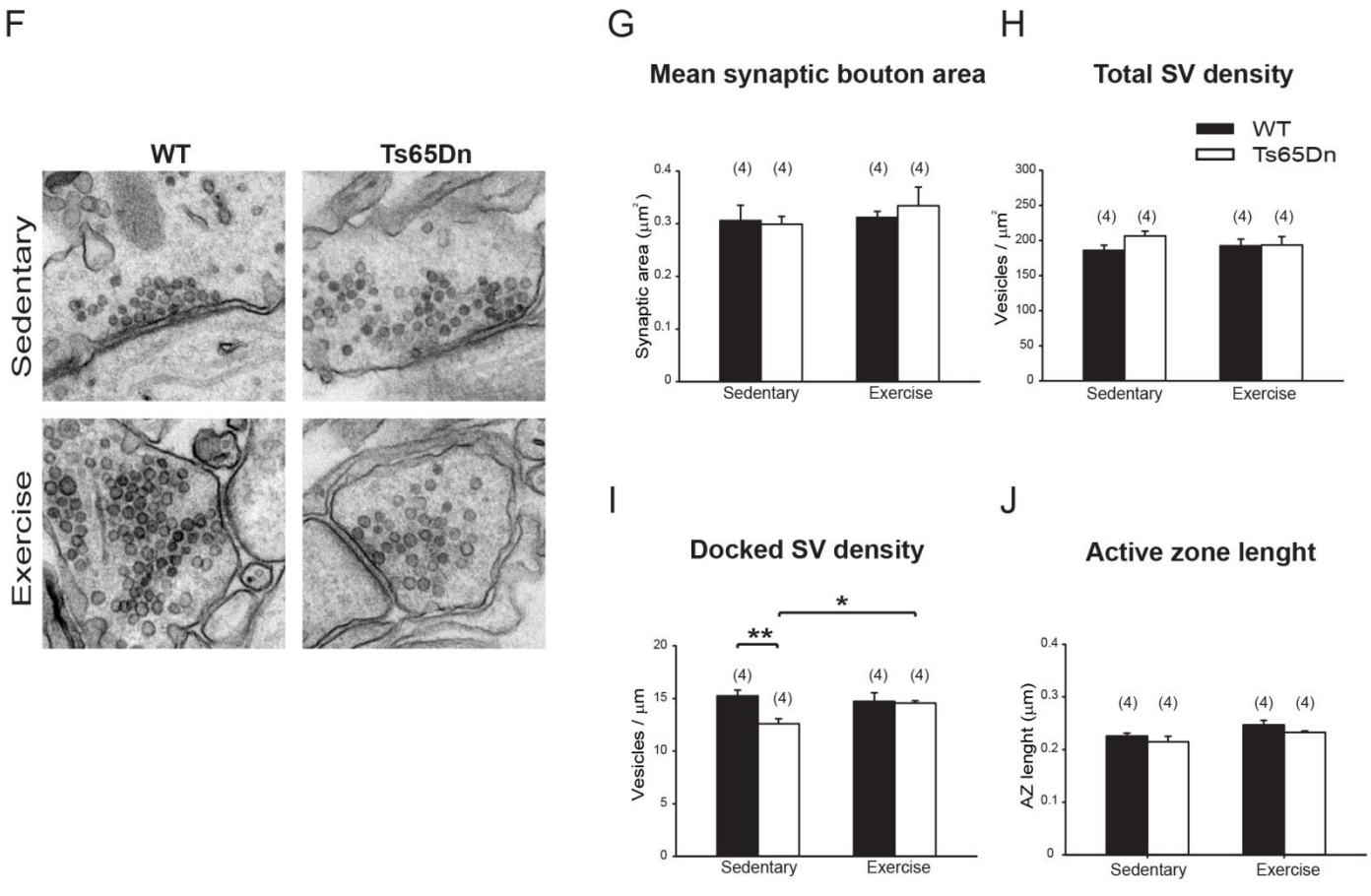

Supplementary Figure 3

Supplementary Figure 3. Synaptic ultrastructural morphometric analysis in the hippocampal CA1 region. **(A)** Representative TEM images showing asymmetric (glutamatergic) synapses. **(B)** Mean asymmetric synaptic bouton area was not significantly different across genotype and treatment. Two-way ANOVA: genotype [$F_{1,15}$=0.108, P=0.748]; treatment [$F_{1,15}$=3.218, P=0.098]; genotype x treatment [$F_{1,15}$=0.097, P=0.761]. **(C)** Total synaptic vesicles (SV) density in asymmetric synapses was not significantly different across genotype and treatment. Two-way ANOVA: genotype [$F_{1,15}$=1.078, P=0.320]; treatment [$F_{1,15}$=1.333, P=0.271]; genotype x treatment [$F_{1,15}$=0.045, P=0.836]. **(D)** The density of docked SV in asymmetric synapses was not significantly different across genotype and treatment. Two-way ANOVA: genotype [$F_{1,15}$=1.797, P=0.205]; treatment [$F_{1,15}$<0.0001, P=0.997]; genotype x treatment [$F_{1,15}$= 0.779, P=0.395]. **(E)** In asymmetric synapses the length of the active zone was increased by exercise in both WT and Ts65Dn mice. Two-way ANOVA: genotype [$F_{1,15}$=1.889, P=0.194]; treatment [$F_{1,15}$=16.940, P=0.001]; genotype x treatment [$F_{1,15}$=0.0745, P=0.790]. **(F)** Representative TEM images showing symmetric (GABAergic) synapses. **(G)** Mean symmetric synaptic bouton area was not significantly different across genotype and treatment. Two-way ANOVA: genotype [$F_{1,15}$=0.0952, P=0.763]; treatment [$F_{1,15}$=0.679, P=0.426]; genotype x treatment [$F_{1,15}$=0.353, P=0.564]. **(H)** Total SV density in symmetric synapses was not significantly different across genotype and treatment. Two-way ANOVA: genotype [$F_{1,15}$=1.379, P=0.263]; treatment [$F_{1,15}$=0.124, P=0.731]; genotype x treatment [$F_{1,15}$=1.145, P=0.306]. **(I)** The density of docked SV in symmetric synapses was reduced in sedentary Ts65Dn mice and significantly restored by exercise. Two-way ANOVA: genotype [$F_{1,15}$=6.265, P=0.028]; treatment [$F_{1,15}$=1.633, P=0.225]; genotype x treatment [$F_{1,15}$=4.922, P=0.047]. **(J)** In symmetric synapses the length of the active zone was not significantly different across genotype and treatment. Two-way ANOVA: genotype [$F_{1,15}$=2.777, P=0.121]; treatment [$F_{1,15}$=6.939, P=0.022]; genotype x treatment [$F_{1,15}$=0.0233, P=0.881]. *P<0.05, **P<0.01, Tukey *post hoc* test following two-way ANOVA. Number in parenthesis indicates the number of mice tested for each experimental group.

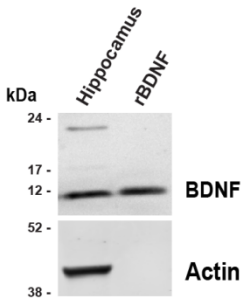

Supplementary Figure 4

Supplementary Figure 4. Specificity of the anti-BDNF antibody used for western blot analysis. Representative immunoblot with anti-BDNF antibody on hippocampal protein extracts or recombinant BDNF (rBDNF). Actin was used as loading control and is absent in rBDNF line.

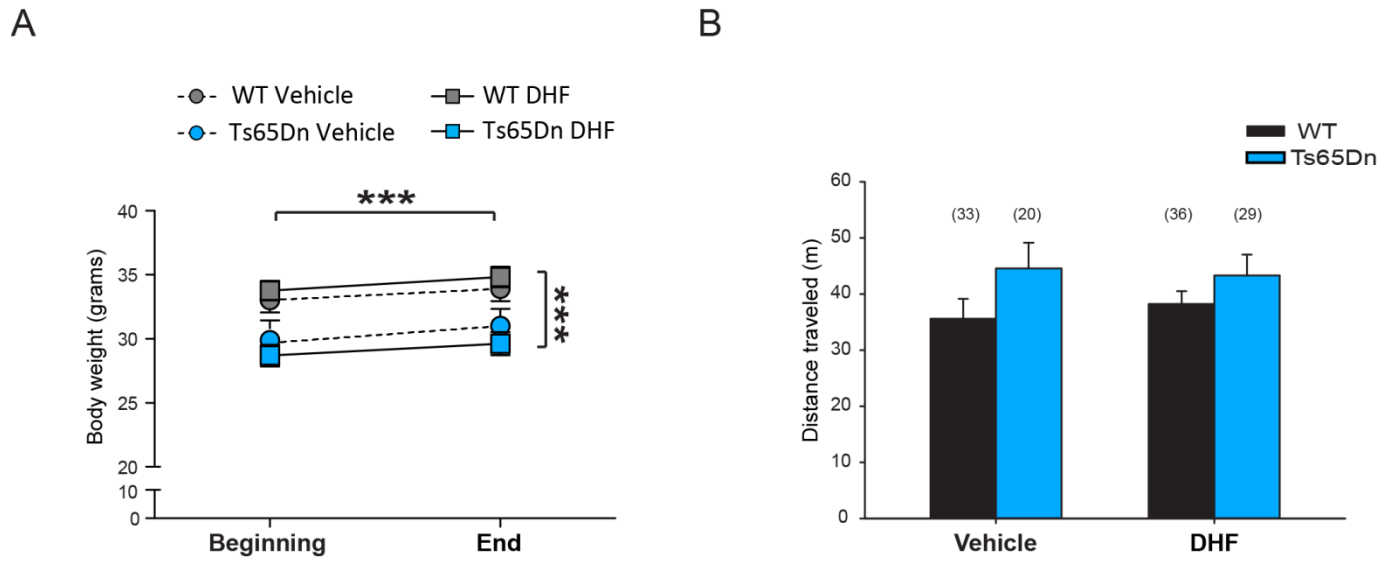

Supplementary Figure 5

Supplementary Figure 5. DHF treatment had no effect on body weight gain and general motor activity. **(A)** Mice body weight was measured at the beginning and at the end (4 weeks later) of chronic DHF or vehicle treatment. As previously reported (Costa, et al. 2010), mean body weight was greater in WT than in Ts65Dn mice (P<0.001). All groups of mice showed comparable and significant weight gain (P<0.001 for all groups) during the 4-week treatment period independently of genotype. Two-way repeated measure ANOVA on ranked-transformed data: genotype [$F_{3,114}$ = 8.509, P < 0.001], time-point [$F_{1,114}$ = 59.318, P < 0.001], genotype x time-point [$F_{3,114}$ = 0.407, P = 0.748]. ***P<0.001, Tukey *post hoc* test. **(B)** Motor activity was evaluated by measuring the distance traveled in the empty arena by mice after chronic DHF or vehicle treatment. Distance traveled was not different across genotype and treatments. Two-way ANOVA: genotype [$F_{1,114}$ = 4.058, P = 0.046], treatment [$F_{1,114}$ = 0.039, P = 0.843], genotype x treatment [$F_{1,114}$ = 0.313, P = 0.577]. Tukey *post hoc* test following two-way ANOVA did not reach statistical significance for any experimental group. Number in parenthesis indicates the number of mice tested for each experimental group.

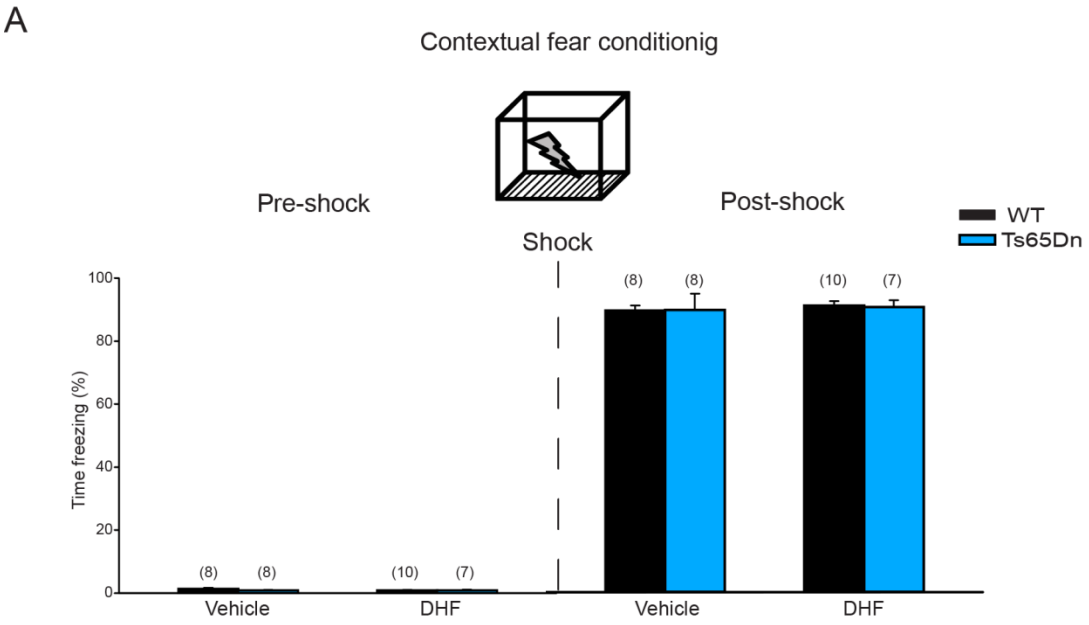

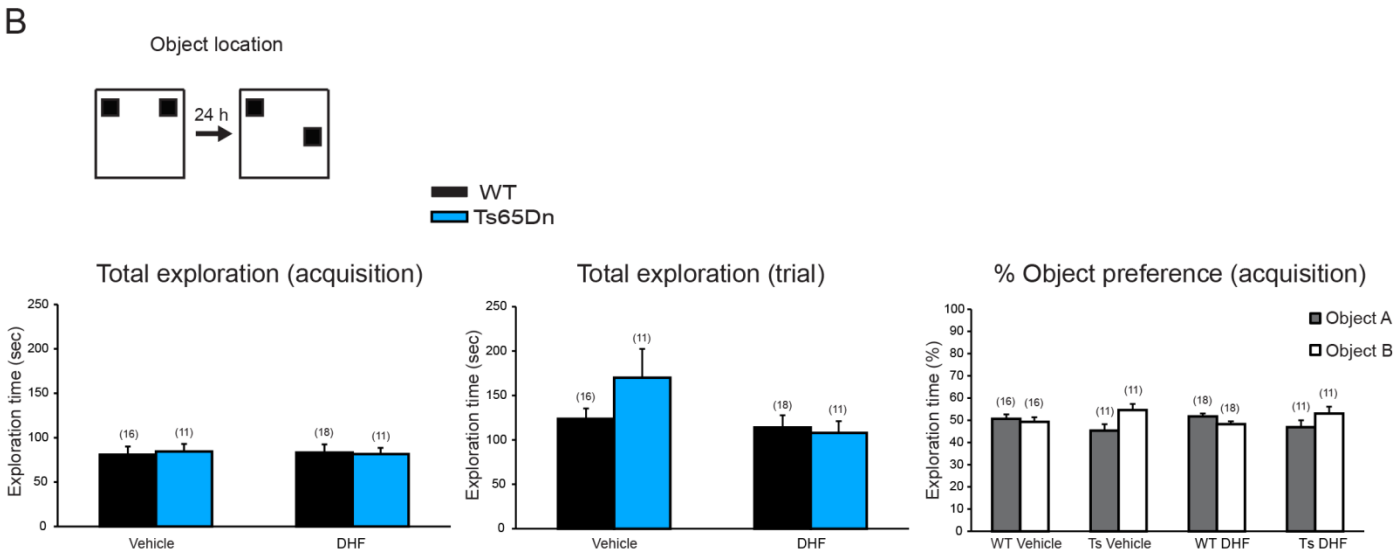

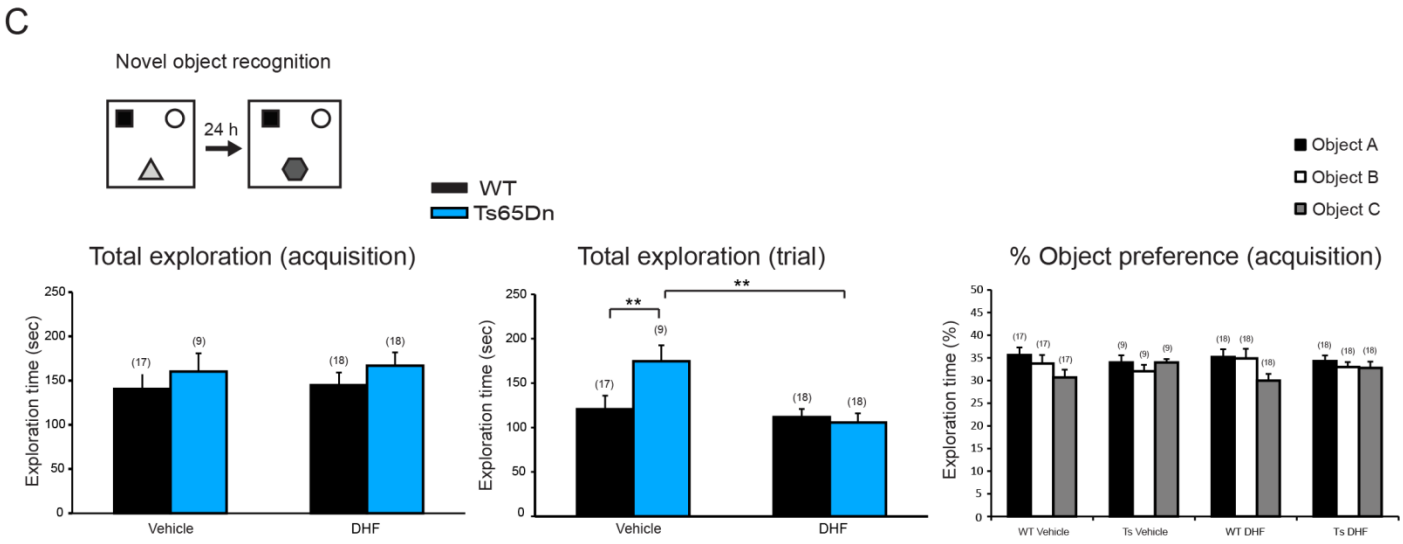

Supplementary Figure 6

Supplementary Figure 6. **(A)** DHF treatment had no effect on the freezing time before (left) or immediately after (right) the electric foot shock during the conditioning session in both Ts65Dn and WT mice. Pre-shock two-way ANOVA: genotype [$F_{1,29}$=1.357, P=0.254]; treatment [$F_{1,29}$=0.505, P=0.483]; genotype x treatment [$F_{1,29}$=1.665, P=0.207]. Post-shock two-way ANOVA: genotype [$F_{1,29}$=0.576, P=0.454]; treatment [$F_{1,29}$=0.140, P=0.711]; genotype x treatment [$F_{1,29}$=2.394, P=0.133]. **(B)** *Left:* in the OL the total exploration time during the acquisition phase was not significantly different across genotype and treatment. Two-way ANOVA: genotype [$F_{1,52}$=0.0084, P=0.927]; treatment [$F_{1,52}$=0.0005, P=0.981]; genotype x treatment [$F_{1,52}$=0.0803, P=0.778]. *Center*: the total exploration time during the trial phase was not significant different across genotype and treatment. Two-way ANOVA: genotype [$F_{1,52}$=0.215, P=0.645]; treatment [$F_{1,52}$=3.764, P=0.058]; genotype x treatment [$F_{1,52}$=0.972, P=0.329]. *Right*: the percentage of time spent exploring the two objects during the acquisition phase was not statistically different across the experimental groups. Two-way ANOVA: genotype [$F_{1,102}$<0.0001, P=1.000]; treatment [$F_{1,102}$=1.108, P=0.349]; genotype x treatment [$F_{1,102}$=2.680, P=0.051]. Number in parenthesis indicates the number of mice tested for each group experimental. **(C)** *Left:* in the NOR test the total exploration time during the acquisition was not significantly different across genotype and treatment. Two-way ANOVA: genotype [$F_{1,58}$=1.526; P=0.222]; treatment [$F_{1,58}$=0.101; P=0.752]; genotype x treatment [$F_{1,58}$=0.0059; P=0.939]. *Center*: the total exploration time during the trial phase was slightly increased in vehicle-treated Ts65Dn mice compared to WT, however no significant difference was observed in Ts65Dn mice treated with DHF compared to WT. Two-way ANOVA: genotype [$F_{1,58}$=3.301; P=0.074]; treatment [$F_{1,58}$=8.720; P=0.005]; genotype x treatment [$F_{1,58}$=5.193; P=0.026]. *Right*: the percentage of time spent exploring the three objects was not statistically different across groups. Two-way ANOVA on ranked transformed data: genotype [$F_{1,174}$=0.110; P=0.741]; treatment [$F_{1,174}$=1.396; P=0.228]; genotype x treatment [$F_{1,174}$=1.141; P=0.340].The number in parenthesis indicate the number of mice tested for each experimental group. **p<0.01, Tukey *post hoc* test following two-way ANOVA.

Full-length blots for Figure 4B

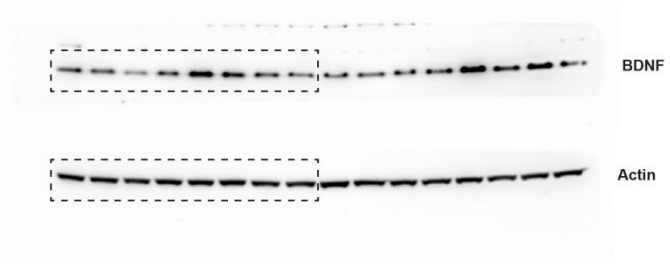

Full-length blots for Figure 5A

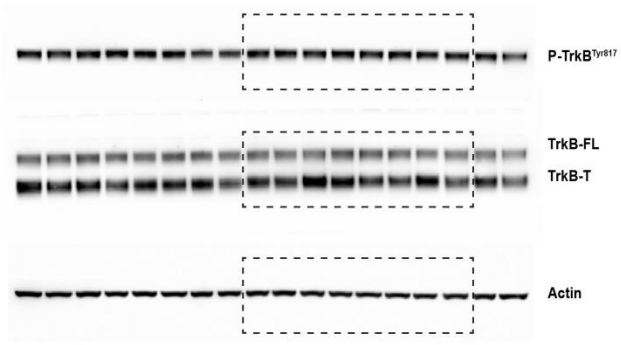

Full-length blots for Figure 5B

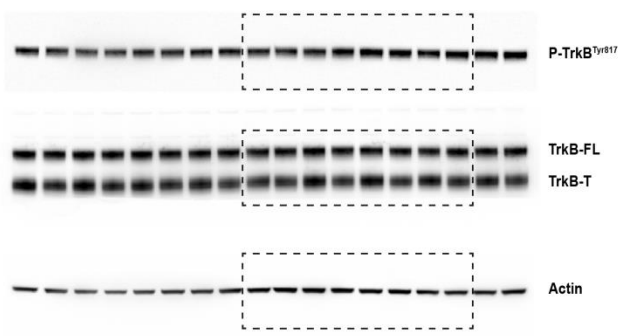

Full-length blots for Figure 5C

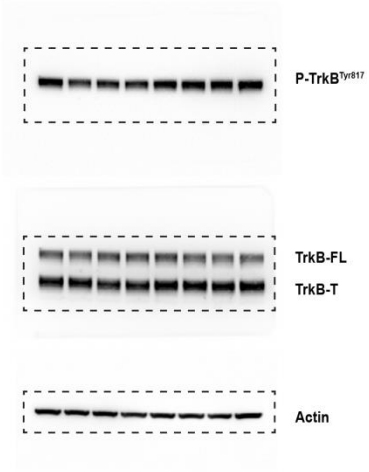

Full-length blots for Figure 5D

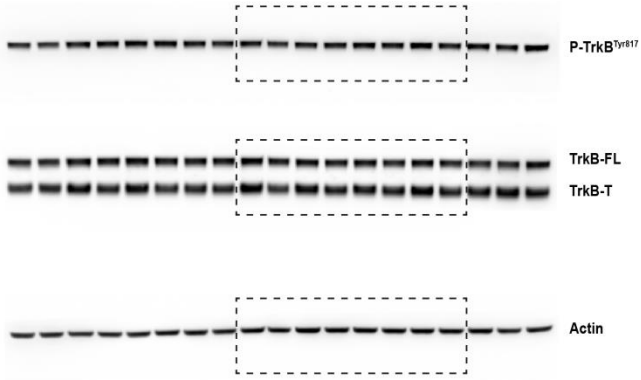

Full-length blots for Figure 7B

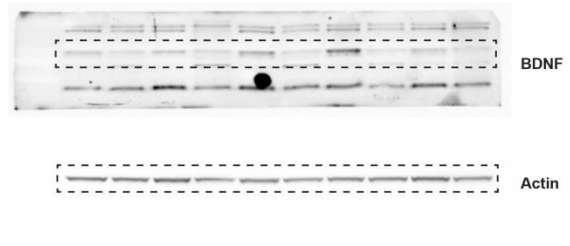

Full-length blots for Supplemenatry Figure 4

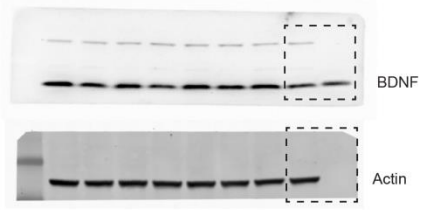

Supplementary Figure 7

Supplementary Fig. 7 Full-length blot images corresponding to the cropped western blot presented in Figure 4, 5, 7 and Supplementary Figure 4.

Supplementary Table 1. Primer sequences for RT-qPCR analysis.

Gene symbol	Gene name	Organism	Accession number	Forward primer (*5′-3′*)	Reverse primer (*5′-3′*)
ACTB	Actin beta	Homo Sapiens	NM_001101	CAGCAAGCAGGAGTATGAC	GAAAGGGTGTAACGCAACT
GAPDH	Glyceraldehyde-3-phosphate dehydrogenase	Homo Sapiens	NM_001256799	AATGAAGGGGTCATTGATGG	AAGGTGAAGGTCGGAGTCAA
PPIA	Peptidylprolyl isomerase A	Homo Sapiens	NM_021130	TTCTGCTGTCTTTGGGACCT	CACCGTGTTCTTCGACATTG
BDNF (CDS)	Brain-derived neurotrophic factor	Homo Sapiens	NM_001143805 NM_001143806 NM_001143807 NM_001143808 NM_001143809 NM_00114381 NM_001143811 NM_00114381 NM_001143814 NM_00114381 NM_001709 NM_170731 NM_170732 NM_170733 NM_170734 NM_170735	CGAGACCAAGTGCAATCC	TTATGAATCGCCAGCCAAT
Actb	Actin beta	Mus Musculus	NM_007393	AAGTGGTTACAGGAAGTCC	ATAATTTACACAGAAGCAATGC
Gapdh	Glyceraldehyde-3-phosphate dehydrogenase	Mus Musculus	NM_008084	GAACATCATCCCTGCATCCA	CCAGTGAGCTTCCCGTTCA
Ppia	Peptidylprolyl isomerase A	Mus Musculus	NM_008907	CACTGTCGCTTTTCGCCGCTTG	TTTCTGCTGTCTTTGGAACTTTGTCTGC
Bdnf (Exon I)	Brain-derived neurotrophic factor	Mus Musculus	NM_007540	TGGTAACCTCGCTCATTCATTAGA	CCCTTCGCAATATCCGCAAAG
Bdnf (Exon II)	Brain-derived neurotrophic factor	Mus Musculus	NM_001048139	CTTTTCCTCGCTGTCAAG	TTGCCAAGAGTCTATTCC
Bdnf (Exon III)	Brain-derived neurotrophic factor	Mus Musculus	NM_001285419	TCACGATCCTCGATGGATAGTTCT	AGGGAGTGGAGCGCAGTC
Bdnf (Exon IV)	Brain-derived neurotrophic factor	Mus Musculus	NM_001048141	CAAATGGAGCTTCTCGCTGAAGGC	GTGGAAATTGCATGGCGGAGGTAA
Bdnf (Exon V)	Brain-derived neurotrophic factor	Mus Musculus	NM_001285420	ACCATAACCCCGCACACTCTGT	GCACCTTCCCGCACCACAAA
Bdnf (Exon VI)	Brain-derived neurotrophic factor	Mus Musculus	NM_001048142	CTTCAACTGCCACCACTG	CATTGTTGTCACGCTTCTG
Bdnf (Exon VII)	Brain-derived neurotrophic factor	Mus Musculus	NM_001285417	GCTTACTTACAGGTCCAAGGTCAA	GTCCTGGAGTTCCGCAGAC
Bdnf (CDS)	Brain-derived neurotrophic factor	Mus Musculus	NM_007540 NM_001048139 NM_001048141 NM_001048142 NM_001285416 NM_001285417 NM_001285418 NM_001285419 NM_001285420 NM_001285421 NM_001285422	ATTACCTGGATGCCGCAAA	TAATACTGTCACACACGCTCA

Supplementary Table 2. Calibration curves parameters, PCR reaction efficiency and amplicon information for RT-qPCR analysis.

Gene symbol	Organism	Amplicon length (bp)	Final primer concentration (µM)	Calibration curve (slope / R^2)	Calculated PCR efficiency (%)	Primer dimers
ACTB	Homo Sapiens	91	0.2	-3.242 / 0.997	103.4	Not detected
GAPDH	Homo Sapiens	108	0.2	-3.493 / 0.999	93.3	Only in NTC samples
PPIA	Homo Sapiens	91	0.2	-3.446 / 0.997	95.1	Not detected
BDNF (CDS)	Homo Sapiens	149	0.2	-3.282 / 0.999	101.7	Not detected
Actb	Mus Musculus	123	0.1	-3.130 / 0.986	108.7	Not detected
Gapdh	Mus Musculus	77	0.2	-3.370 / 0.999	98.0	Only in NTC samples
Ppia	Mus Musculus	133	0.2	-3.321 / 0.994	100.0	Only in NTC samples
Bdnf (Exon I)	Mus Musculus	172	0.2	-3.450 / 0.999	94.9	Not detected
Bdnf (Exon II)	Mus Musculus	200	0.1	-3.175 / 0.998	106.5	Not detected
Bdnf (Exon III)	Mus Musculus	150	0.2	-3.716 / 0.994	85.3	Not detected
Bdnf (Exon IV)	Mus Musculus	57	0.2	-3.584 / 0.999	90.1	Not detected
Bdnf (Exon V)	Mus Musculus	73	0.2	-3.536 / 0.997	91.8	Not detected
Bdnf (Exon VI)	Mus Musculus	87	0.2	-3.573 / 0.999	90.5	Only in NTC samples
Bdnf (Exon VII)	Mus Musculus	93	0.2	-3.503 / 0.996	92.9	Not detected
Bdnf (CDS)	Mus Musculus	90	0.2	-3.315 / 0.999	100.3	Not detected

Supplementary Table 3. Human sample information.

Case number	Disorder	Age (years)	Gender
1276	DS	13	M
5277	DS	19	M
M1960M	DS	19	M
5341	DS	25	M
5005	DS	39	F
4925	Control	13	M
4782	Control	18	M
1841	Control	19	M
605	Control	25	M
5606	Control	35	F

Supplementary Table 4. List of mice used in the study.

			Behavior			IHC					
Mouse #	Genotype	Treatment	NOR	OL	CFC	BrdU 24hr	BrdU 4w	VGAT/VGLUT1	EPhy	EF	Bioch
1	WT	sedentary	*			*		*			
2	WT	sedentary	*			*					
3	WT	sedentary	*			*					
4	WT	sedentary	*			*					
5	WT	sedentary	*			*					
6	WT	sedentary	*			*		*			
7	WT	sedentary	*				*				
8	WT	sedentary	*				*				
9	WT	sedentary	*				*				
10	WT	sedentary	*				*	*	*		
11	WT	sedentary	*				*	*	*		
12	WT	sedentary	*				*				
13	WT	sedentary	*				*	*	*		
14	WT	sedentary	*				*	*	*		
15	WT	sedentary	*				*				
16	WT	sedentary	*				*				
17	WT	sedentary	*								
18	WT	sedentary	*								
19	WT	sedentary	*								
20	WT	sedentary	*								
21	WT	sedentary	*								

22	WT	sedentary	*								
23	WT	sedentary	*								
24	WT	sedentary	*								
25	WT	sedentary	*								
26	WT	sedentary	*								
27	WT	sedentary	*								
28	WT	sedentary	*								
29	WT	sedentary			*						
30	WT	sedentary			*						
31	WT	sedentary			*						
32	WT	sedentary			*						
33	WT	sedentary			*						
34	WT	sedentary			*						
35	WT	sedentary			*						
36	WT	sedentary			*						
37	WT	sedentary			*						
38	WT	sedentary			*						
39	WT	sedentary			*						
40	WT	sedentary			*						
41	WT	sedentary			*						
42	WT	sedentary			*						
43	WT	sedentary		*							
44	WT	sedentary		*							
45	WT	sedentary		*							
46	WT	sedentary		*							
47	WT	sedentary		*							
48	WT	sedentary		*							
49	WT	sedentary		*							
50	WT	sedentary		*							
51	WT	sedentary		*							
52	WT	sedentary		*							
53	WT	sedentary		*							
54	WT	sedentary		*							
55	WT	sedentary		*							
56	WT	sedentary		*							
57	WT	sedentary		*							
58	WT	sedentary		*							
59	WT	sedentary		*							
60	WT	sedentary		*							
61	WT	sedentary		*							
62	WT	sedentary		*							
63	WT	sedentary		*							
64	WT	sedentary								*	
65	WT	sedentary								*	
66	WT	sedentary								*	
67	WT	sedentary								*	
68	WT	sedentary								*	

69	WT	sedentary								*	
70	WT	sedentary								*	
71	WT	sedentary								*	
72	WT	sedentary								*	
73	WT	sedentary								*	
74	WT	sedentary								*	
75	WT	sedentary								*	
76	WT	sedentary								*	
77	WT	sedentary								*	
78	WT	sedentary								*	
79	WT	sedentary								*	
80	WT	sedentary									*
81	WT	sedentary									*
82	WT	sedentary									*
83	WT	sedentary									*
84	WT	sedentary									*
85	WT	sedentary									*
86	WT	sedentary									*
87	WT	sedentary									*
88	WT	sedentary									*
89	WT	sedentary									*
90	WT	sedentary									*
91	WT	sedentary									*
92	Ts65Dn	sedentary	*			*					
93	Ts65Dn	sedentary	*			*		*	*		
94	Ts65Dn	sedentary	*			*					
95	Ts65Dn	sedentary	*			*		*			
96	Ts65Dn	sedentary	*			*		*	*		
97	Ts65Dn	sedentary	*			*					
98	Ts65Dn	sedentary	*			*		*			
99	Ts65Dn	sedentary	*				*	*	*		
100	Ts65Dn	sedentary	*				*	*	*		
101	Ts65Dn	sedentary	*				*	*			
102	Ts65Dn	sedentary	*				*	*			
103	Ts65Dn	sedentary	*				*	*			
104	Ts65Dn	sedentary	*								
105	Ts65Dn	sedentary	*								
106	Ts65Dn	sedentary	*								
107	Ts65Dn	sedentary	*								
108	Ts65Dn	sedentary	*								
109	Ts65Dn	sedentary			*						
110	Ts65Dn	sedentary			*						
111	Ts65Dn	sedentary			*						
112	Ts65Dn	sedentary			*						
113	Ts65Dn	sedentary			*						
114	Ts65Dn	sedentary			*						
115	Ts65Dn	sedentary			*						

116	Ts65Dn	sedentary		*	*						
117	Ts65Dn	sedentary		*							
118	Ts65Dn	sedentary		*							
119	Ts65Dn	sedentary		*							
120	Ts65Dn	sedentary		*							
121	Ts65Dn	sedentary		*							
122	Ts65Dn	sedentary		*							
123	Ts65Dn	sedentary		*							
124	Ts65Dn	sedentary		*							
125	Ts65Dn	sedentary		*							
126	Ts65Dn	sedentary		*							
127	Ts65Dn	sedentary		*							
128	Ts65Dn	sedentary								*	
129	Ts65Dn	sedentary								*	
130	Ts65Dn	sedentary								*	
131	Ts65Dn	sedentary								*	
132	Ts65Dn	sedentary								*	
133	Ts65Dn	sedentary								*	
134	Ts65Dn	sedentary								*	
135	Ts65Dn	sedentary								*	
136	Ts65Dn	sedentary								*	
137	Ts65Dn	sedentary								*	
138	Ts65Dn	sedentary								*	
139	Ts65Dn	sedentary								*	
140	Ts65Dn	sedentary									*
141	Ts65Dn	sedentary									*
142	Ts65Dn	sedentary									*
143	Ts65Dn	sedentary									*
144	Ts65Dn	sedentary									*
145	Ts65Dn	sedentary									*
146	Ts65Dn	sedentary									*
147	Ts65Dn	sedentary									*
148	Ts65Dn	sedentary									*
149	Ts65Dn	sedentary									*
150	Ts65Dn	sedentary									*
151	Ts65Dn	sedentary									*
152	WT	exercise	*			*					
153	WT	exercise	*			*					
154	WT	exercise	*			*					
155	WT	exercise	*			*		*			
156	WT	exercise	*			*					
157	WT	exercise	*			*					
158	WT	exercise	*			*		*	*		
159	WT	exercise	*			*		*			
160	WT	exercise	*				*	*			
161	WT	exercise	*				*	*			
162	WT	exercise	*				*				

163	WT	exercise	*				*				
164	WT	exercise		*			*	*	*		
165	WT	exercise		*			*	*	*		
166	WT	exercise		*			*				
167	WT	exercise		*			*				
168	WT	exercise		*			*	*	*		
169	WT	exercise	*								
170	WT	exercise	*								
171	WT	exercise			*						
172	WT	exercise			*						
173	WT	exercise			*						
174	WT	exercise			*						
175	WT	exercise			*						
176	WT	exercise			*						
177	WT	exercise			*						
178	WT	exercise			*						
179	WT	exercise			*						
180	WT	exercise			*						
181	WT	exercise			*						
182	WT	exercise			*						
183	WT	exercise			*						
184	WT	exercise			*						
185	WT	exercise			*						
186	WT	exercise			*						
187	WT	exercise		*							
188	WT	exercise		*							
189	WT	exercise		*							
190	WT	exercise		*							
191	WT	exercise		*							
192	WT	exercise		*							
193	WT	exercise		*							
194	WT	exercise		*							
195	WT	exercise		*							
196	WT	exercise		*							
197	WT	exercise		*							
198	WT	exercise		*							
199	WT	exercise								*	
200	WT	exercise								*	
201	WT	exercise								*	
202	WT	exercise								*	
203	WT	exercise								*	
204	WT	exercise								*	
205	WT	exercise								*	
206	WT	exercise								*	
207	WT	exercise								*	
208	WT	exercise								*	
209	WT	exercise								*	

210	WT	exercise								*	
211	WT	exercise									*
212	WT	exercise									*
213	WT	exercise									*
214	WT	exercise									*
215	WT	exercise									*
216	WT	exercise									*
217	WT	exercise									*
218	WT	exercise									*
219	WT	exercise									*
220	WT	exercise									*
221	WT	exercise									*
222	WT	exercise									*
223	Ts65Dn	exercise	*			*					
224	Ts65Dn	exercise	*			*					
225	Ts65Dn	exercise	*			*		*			
226	Ts65Dn	exercise	*			*					
227	Ts65Dn	exercise	*			*					
228	Ts65Dn	exercise	*			*		*			
229	Ts65Dn	exercise	*				*	*	*		
230	Ts65Dn	exercise	*				*				
231	Ts65Dn	exercise		*			*				
232	Ts65Dn	exercise	*				*	*	*		
233	Ts65Dn	exercise	*				*	*	*		
234	Ts65Dn	exercise		*			*	*	*		
235	Ts65Dn	exercise		*			*				
236	Ts65Dn	exercise	*								
237	Ts65Dn	exercise	*								
238	Ts65Dn	exercise	*								
239	Ts65Dn	exercise	*								
240	Ts65Dn	exercise	*								
241	Ts65Dn	exercise	*								
242	Ts65Dn	exercise	*								
243	Ts65Dn	exercise			*						
244	Ts65Dn	exercise			*						
245	Ts65Dn	exercise			*						
246	Ts65Dn	exercise			*						
247	Ts65Dn	exercise			*						
248	Ts65Dn	exercise			*						
249	Ts65Dn	exercise			*						
250	Ts65Dn	exercise			*						
251	Ts65Dn	exercise			*						
252	Ts65Dn	exercise		*	*						
253	Ts65Dn	exercise		*	*						
254	Ts65Dn	exercise		*							
255	Ts65Dn	exercise		*							
256	Ts65Dn	exercise		*							

257	Ts65Dn	exercise		*							
258	Ts65Dn	exercise		*							
259	Ts65Dn	exercise		*							
260	Ts65Dn	exercise		*							
261	Ts65Dn	exercise		*							
262	Ts65Dn	exercise								*	
263	Ts65Dn	exercise								*	
264	Ts65Dn	exercise								*	
265	Ts65Dn	exercise								*	
266	Ts65Dn	exercise								*	
267	Ts65Dn	exercise								*	
268	Ts65Dn	exercise								*	
269	Ts65Dn	exercise								*	
270	Ts65Dn	exercise								*	
271	Ts65Dn	exercise								*	
272	Ts65Dn	exercise								*	
273	Ts65Dn	exercise								*	
274	Ts65Dn	exercise									*
275	Ts65Dn	exercise									*
276	Ts65Dn	exercise									*
277	Ts65Dn	exercise									*
278	Ts65Dn	exercise									*
279	Ts65Dn	exercise									*
280	Ts65Dn	exercise									*
281	Ts65Dn	exercise									*
282	Ts65Dn	exercise									*
283	Ts65Dn	exercise									*
284	Ts65Dn	exercise									*
285	Ts65Dn	exercise									*
286	WT	vehicle	*								
287	WT	vehicle	*								
288	WT	vehicle	*								
289	WT	vehicle	*								
290	WT	vehicle	*								
291	WT	vehicle	*								
292	WT	vehicle	*		*						
293	WT	vehicle	*		*						
294	WT	vehicle	*		*						
295	WT	vehicle	*		*						
296	WT	vehicle	*		*						
297	WT	vehicle	*		*						
298	WT	vehicle	*		*						
299	WT	vehicle	*		*						
300	WT	vehicle	*								
301	WT	vehicle	*								
302	WT	vehicle	*								
303	WT	vehicle		*							
304	WT	vehicle		*							

305	WT	vehicle		*							
306	WT	vehicle		*							
307	WT	vehicle		*							
308	WT	vehicle		*							
309	WT	vehicle		*							
310	WT	vehicle		*							
311	WT	vehicle		*							
312	WT	vehicle		*							
313	WT	vehicle		*							
314	WT	vehicle		*							
315	WT	vehicle		*							
316	WT	vehicle		*							
317	WT	vehicle		*							
318	WT	vehicle		*							
319	WT	vehicle								*	
320	WT	vehicle								*	
321	WT	vehicle								*	
322	WT	vehicle								*	
323	WT	vehicle								*	
324	WT	vehicle								*	
325	WT	vehicle									*
326	WT	vehicle									*
327	WT	vehicle									*
328	WT	vehicle									*
329	WT	vehicle									*
330	WT	vehicle									*
331	WT	vehicle									*
332	WT	vehicle									*
333	WT	vehicle									*
334	WT	vehicle									*
335	WT	vehicle									*
336	WT	vehicle									*
337	WT	vehicle (acute)									*
338	WT	vehicle (acute)									*
339	WT	vehicle (acute)									*
340	WT	vehicle (acute)									*
341	WT	vehicle (acute)									*
342	WT	vehicle (acute)									*
343	WT	vehicle (acute)									*
344	WT	vehicle (acute)									*
345	WT	vehicle (acute)									*
346	WT	vehicle (acute)									*
347	WT	vehicle (acute)									*
348	WT	vehicle (acute)									*
349	WT	vehicle (acute)									*
350	WT	vehicle (acute)									*
351	WT	vehicle (acute)									*
352	WT	vehicle (acute)									*
353	Ts65Dn	vehicle	*		*						

354	Ts65Dn	vehicle	*		*						
355	Ts65Dn	vehicle	*		*						
356	Ts65Dn	vehicle	*		*						
357	Ts65Dn	vehicle	*		*						
358	Ts65Dn	vehicle	*		*						
359	Ts65Dn	vehicle	*		*						
360	Ts65Dn	vehicle	*		*						
361	Ts65Dn	vehicle	*								
362	Ts65Dn	vehicle		*							
363	Ts65Dn	vehicle		*							
364	Ts65Dn	vehicle		*							
365	Ts65Dn	vehicle		*							
366	Ts65Dn	vehicle		*							
367	Ts65Dn	vehicle		*							
368	Ts65Dn	vehicle		*							
369	Ts65Dn	vehicle		*							
370	Ts65Dn	vehicle		*							
371	Ts65Dn	vehicle		*							
372	Ts65Dn	vehicle		*							
373	Ts65Dn	vehicle								*	
374	Ts65Dn	vehicle								*	
375	Ts65Dn	vehicle									*
376	Ts65Dn	vehicle									*
377	Ts65Dn	vehicle									*
378	Ts65Dn	vehicle									*
379	Ts65Dn	vehicle									*
380	Ts65Dn	vehicle									*
381	Ts65Dn	vehicle									*
382	Ts65Dn	vehicle									*
383	Ts65Dn	vehicle									*
384	Ts65Dn	vehicle									*
385	Ts65Dn	vehicle									*
386	Ts65Dn	vehicle									*
387	Ts65Dn	vehicle (acute)									*
388	Ts65Dn	vehicle (acute)									*
389	Ts65Dn	vehicle (acute)									*
390	Ts65Dn	vehicle (acute)									*
391	Ts65Dn	vehicle (acute)									*
392	Ts65Dn	vehicle (acute)									*
393	Ts65Dn	vehicle (acute)									*
394	Ts65Dn	vehicle (acute)									*
395	Ts65Dn	vehicle (acute)									*
396	Ts65Dn	vehicle (acute)									*
397	Ts65Dn	vehicle (acute)									*
398	Ts65Dn	vehicle (acute)									*
399	Ts65Dn	vehicle (acute)									*
400	Ts65Dn	vehicle (acute)									*
401	Ts65Dn	vehicle (acute)									*
402	Ts65Dn	vehicle (acute)									*

403	WT	DHF	*								
404	WT	DHF	*								
405	WT	DHF	*								
406	WT	DHF	*								
407	WT	DHF	*								
408	WT	DHF	*		*						
409	WT	DHF	*		*						
410	WT	DHF	*		*						
411	WT	DHF	*								
412	WT	DHF	*		*						
413	WT	DHF	*		*						
414	WT	DHF	*		*						
415	WT	DHF	*		*						
416	WT	DHF	*		*						
417	WT	DHF	*		*						
418	WT	DHF	*								
419	WT	DHF	*								
420	WT	DHF	*								
421	WT	DHF			*						
422	WT	DHF		*							
423	WT	DHF		*							
424	WT	DHF		*							
425	WT	DHF		*							
426	WT	DHF		*							
427	WT	DHF		*							
428	WT	DHF		*							
429	WT	DHF		*							
430	WT	DHF		*							
431	WT	DHF		*							
432	WT	DHF		*							
433	WT	DHF		*							
434	WT	DHF		*							
435	WT	DHF		*							
436	WT	DHF		*							
437	WT	DHF		*							
438	WT	DHF		*							
439	WT	DHF		*							
440	WT	DHF								*	
441	WT	DHF								*	
442	WT	DHF								*	
443	WT	DHF								*	
444	WT	DHF									*
445	WT	DHF									*
446	WT	DHF									*
447	WT	DHF									*
448	WT	DHF									*
449	WT	DHF									*
450	WT	DHF									*
451	WT	DHF									*

452	WT	DHF									*
453	WT	DHF									*
454	WT	DHF									*
455	WT	DHF									*
456	WT	DHF (acute)									*
457	WT	DHF (acute)									*
458	WT	DHF (acute)									*
459	WT	DHF (acute)									*
460	WT	DHF (acute)									*
461	WT	DHF (acute)									*
462	WT	DHF (acute)									*
463	WT	DHF (acute)									*
464	WT	DHF (acute)									*
465	WT	DHF (acute)									*
466	WT	DHF (acute)									*
467	WT	DHF (acute)									*
468	WT	DHF (acute)									*
469	WT	DHF (acute)									*
470	WT	DHF (acute)									*
471	WT	DHF (acute)									*
472	WT	DHF (acute)									*
473	WT	DHF (acute)									*
474	WT	DHF (acute)									*
475	WT	DHF (acute)									*
476	Ts65Dn	DHF	*								
477	Ts65Dn	DHF	*								
478	Ts65Dn	DHF	*								
479	Ts65Dn	DHF	*								
480	Ts65Dn	DHF	*								
481	Ts65Dn	DHF	*								
482	Ts65Dn	DHF	*								
483	Ts65Dn	DHF	*								
484	Ts65Dn	DHF	*		*						
485	Ts65Dn	DHF	*		*						
486	Ts65Dn	DHF	*		*						
487	Ts65Dn	DHF	*		*						
488	Ts65Dn	DHF	*		*						
489	Ts65Dn	DHF	*		*						
490	Ts65Dn	DHF	*		*						
491	Ts65Dn	DHF	*								
492	Ts65Dn	DHF	*								
493	Ts65Dn	DHF	*								
494	Ts65Dn	DHF		*							
495	Ts65Dn	DHF		*							
496	Ts65Dn	DHF		*							
497	Ts65Dn	DHF		*							
498	Ts65Dn	DHF		*							
499	Ts65Dn	DHF		*							
500	Ts65Dn	DHF		*							

501	Ts65Dn	DHF		*							
502	Ts65Dn	DHF		*							
503	Ts65Dn	DHF		*							
504	Ts65Dn	DHF		*							
505	Ts65Dn	DHF								*	
506	Ts65Dn	DHF								*	
507	Ts65Dn	DHF								*	
508	Ts65Dn	DHF									*
509	Ts65Dn	DHF									*
510	Ts65Dn	DHF									*
511	Ts65Dn	DHF									*
512	Ts65Dn	DHF									*
513	Ts65Dn	DHF									*
514	Ts65Dn	DHF									*
515	Ts65Dn	DHF									*
516	Ts65Dn	DHF									*
517	Ts65Dn	DHF									*
518	Ts65Dn	DHF									*
519	Ts65Dn	DHF									*
520	Ts65Dn	DHF (acute)									*
521	Ts65Dn	DHF (acute)									*
522	Ts65Dn	DHF (acute)									*
523	Ts65Dn	DHF (acute)									*
524	Ts65Dn	DHF (acute)									*
525	Ts65Dn	DHF (acute)									*
526	Ts65Dn	DHF (acute)									*
527	Ts65Dn	DHF (acute)									*
528	Ts65Dn	DHF (acute)									*
529	Ts65Dn	DHF (acute)									*
530	Ts65Dn	DHF (acute)									*
531	Ts65Dn	DHF (acute)									*
532	Ts65Dn	DHF (acute)									*
533	Ts65Dn	DHF (acute)									*
534	Ts65Dn	DHF (acute)									*
535	Ts65Dn	DHF (acute)									*
536	Ts65Dn	DHF (acute)									*
537	Ts65Dn	DHF (acute)									*
538	Ts65Dn	DHF (acute)									*
539	Ts65Dn	DHF (acute)									*

Asterisk indicates the experimental procedure/test carried out on each mouse.
NOR: Novel Object Recognition test. OL: Object Location test. CFC: Contextual Fear Conditioning test. IHC: Immunohistochemistry. EM: Electron Microscopy. EPhy: Electrophysiology. Bioch: Biochemistry.
Mice highlighted in yellow did perform the NOR or OL behavioral tests, but could not be included in the study because we lost the video-recording files of the behavioral tests due to the failure of a hard-drive in which they were stored. Files could not be recovered.

Supplementary references

Costa, A. C. S., M. R. Stasko, C. Schmidt and M. T. Davisson (2010). "Behavioral validation of the Ts65Dn mouse model for Down syndrome of a genetic background free of the retinal degeneration mutation Pde6brd1." Behavioural Brain Research **206**: 52-62.